NAVAL POSTGRADUATE SCHOOL

MONTEREY, CALIFORNIA

THESIS

HALO ORBIT DESIGN AND OPTIMIZATION

by

Gina McCaine

March 2004

Thesis Advisor:	I. Michael Ross
Co-Thesis Advisor:	Don Danielson

Approved for public release; distribution is unlimited.

THIS PAGE INTENTIONALLY LEFT BLANK

REPORT DOCUMENTATION PAGE				*Form Approved OMB No. 0704-0188*
Public reporting burden for this collection of information is estimated to average 1 hour per response, including the time for reviewing instruction, searching existing data sources, gathering and maintaining the data needed, and completing and reviewing the collection of information. Send comments regarding this burden estimate or any other aspect of this collection of information, including suggestions for reducing this burden, to Washington headquarters Services, Directorate for Information Operations and Reports, 1215 Jefferson Davis Highway, Suite 1204, Arlington, VA 22202-4302, and to the Office of Management and Budget, Paperwork Reduction Project (0704-0188) Washington DC 20503.				
1. AGENCY USE ONLY *(Leave blank)*	**2. REPORT DATE** March 2004	**3. REPORT TYPE AND DATES COVERED** Master's Thesis		
4. TITLE AND SUBTITLE: Halo Orbit Design and Optimization				**5. FUNDING NUMBERS**
6. AUTHOR(S) Gina McCaine				
7. PERFORMING ORGANIZATION NAME(S) AND ADDRESS(ES) Naval Postgraduate School Monterey, CA 93943-5000				**8. PERFORMING ORGANIZATION REPORT NUMBER**
9. SPONSORING /MONITORING AGENCY NAME(S) AND ADDRESS(ES) N/A				**10. SPONSORING/MONITORING AGENCY REPORT NUMBER**
11. SUPPLEMENTARY NOTES The views expressed in this thesis are those of the author and do not reflect the official policy or position of the Department of Defense or the U.S. Government.				
12a. DISTRIBUTION / AVAILABILITY STATEMENT Approved for public release; distribution unlimited				**12b. DISTRIBUTION CODE**

13. ABSTRACT (maximum 200 words)

A Halo orbit about a libration point of a restricted three-body system provides additional opportunities for surveillance, communication, and exploratory missions in lieu of the classical spacecraft orbit. Historically libration point missions have focused on Halo orbits and trajectories about the Sun-Earth System. This thesis will focus on libration point orbit solutions in the Earth-Moon system using the restricted three body equations of motion with three low-thrust control functions. These classical dynamics are used to design and optimize orbital trajectories about stable and unstable libration points of the Earth-Moon system using DIDO, a dynamic optimization software. The solutions for the optimized performance are based on a quadratic cost function. Specific constraints and bounds were placed on the potential solution set in order to ensure correct target trajectories. This approach revealed locally optimal solutions for orbits about a stable and unstable libration point.

14. SUBJECT TERMS Halo orbit, DIDO, Lagrange Point, Libration Point, Optimization			**15. NUMBER OF PAGES** 56
			16. PRICE CODE
17. SECURITY CLASSIFICATION OF REPORT Unclassified	**18. SECURITY CLASSIFICATION OF THIS PAGE** Unclassified	**19. SECURITY CLASSIFICATION OF ABSTRACT** Unclassified	**20. LIMITATION OF ABSTRACT** UL

NSN 7540-01-280-5500 Standard Form 298 (Rev. 2-89)
Prescribed by ANSI Std. 239-18

THIS PAGE INTENTIONALLY LEFT BLANK

Approved for public release; distribution is unlimited.

HALO ORBIT DESIGN AND OPTIMIZATION

Gina L. McCaine
Lieutenant, United States Navy
B.S., United States Naval Academy, 1997

Submitted in partial fulfillment of the
requirements for the degree of

MASTER OF SCIENCE IN ASTRONAUTICAL ENGINEERING

from the

NAVAL POSTGRADUATE SCHOOL
March 2004

Author: Gina L. McCaine

Approved by: I. Michael Ross
Thesis Advisor

Don Danielson
Co-Thesis Advisor/Second Reader

Anthony Healey
Chairman, Department of Mechanical and Astronautical Engineering

THIS PAGE INTENTIONALLY LEFT BLANK

ABSTRACT

A Halo orbit about a libration point of a restricted three-body system provides additional opportunities for surveillance, communication, and exploratory missions in lieu of the classical spacecraft orbit. Historically libration point missions have focused on Halo orbits and trajectories about the Sun-Earth System. This thesis will focus on libration point orbit solutions in the Earth-Moon system using the restricted three body equations of motion with three low-thrust control functions. These classical dynamics are used to design and optimize orbital trajectories about stable and unstable libration points of the Earth-Moon system using DIDO, a dynamic optimization software. The solutions for the optimized performance are based on a quadratic cost function. Specific constraints and bounds were placed on the potential solution set in order to ensure correct target trajectories. This approach revealed locally optimal solutions for orbits about a stable and unstable libration point.

THIS PAGE INTENTIONALLY LEFT BLANK

TABLE OF CONTENTS

THIS PAGE INTENTIONALLY LEFT BLANK

LIST OF FIGURES

THIS PAGE INTENTIONALLY LEFT BLANK

LIST OF TABLES

THIS PAGE INTENTIONALLY LEFT BLANK

ACKNOWLEDGMENTS

For God and Country.

I. INTRODUCTION

Libration points, also referred to as Lagrange points in the literature [Refs 1-16], represent equilibrium positions in the restricted three-body problem. Of the five libration points, two points, L4 and L5, are stable, meaning that it is possible for a spacecraft to remain stationary at that point or orbit about it. The co-linear Lagrange points L1, L2, and L3 are unstable; yet provide a sensitive region of stability about which a spacecraft may orbit. All points are referenced from the barycenter ('B') of the system, which defines the origin in the reference frame and represents the mass center of the system. Figure 1 illustrates the positioning of the libration points for the Sun-Earth system, and

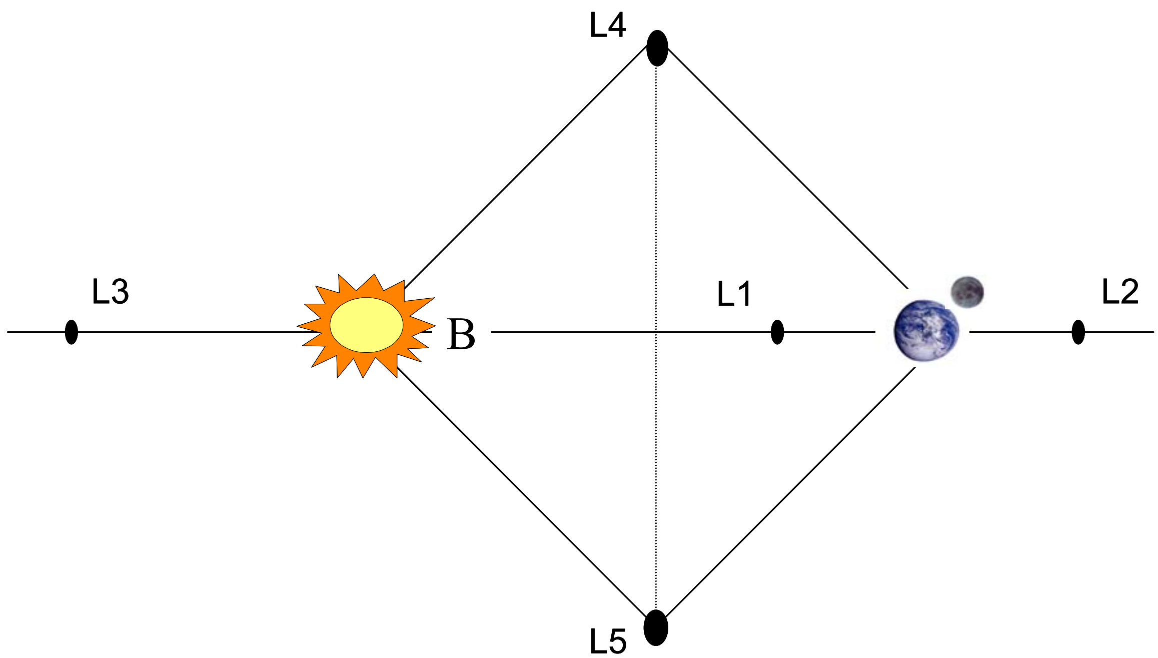

Figure 1. Sun-Earth Libration Point System

the convention that shall be used to identify each point throughout this thesis. In this figure, the Sun represents the primary body of the system, and the secondary body in the Earth.

The most common type of orbit about a libration point is generally referred to as a Halo orbit [Refs 1-12], and provides addition opportunities for surveillance, communications or exploratory missions. Halo is not an acronym, the orbit is so named because the orbital plane does not intersect the main celestial body as a classical orbit does. Instead, the orbit resembles a Halo hovering overhead as shown in Figure 2. The advantage of this type of orbit over the traditional orbit is that it generally provides a continuous and uninterrupted view of its mission subject.

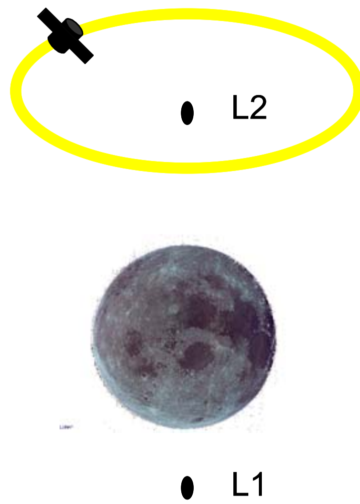

Figure 2. HALO Orbit about L2 Point of Earth-Moon System

The purpose of this thesis is to design an optimal Halo orbit about a libration point of the Earth-Moon system, using the DIDO optimization software, which is a MATLAB application tool. This optimal solution method may be additionally applied to any general three-body system, and at the appropriate libration point. All libration missions to date have been in the Sun-Earth System. This thesis will attempt to exploit the Earth Moon-System for a future communications satellite mission.

The design criteria or specifications for the libration point orbits in this thesis are based on orbital period, bounds, and constraints particular to the Earth-Moon system. This problem is scaled and non-dimensionalized, however different masses yield unique mass ratios between the primary and secondary bodies, and alter the dynamics and boundary conditions of the problem with respect to libration point location and orbit optimization. Therefore, the characteristics of the system as well as target orbits are important in shaping the design process.

II. BACKGROUND

In the history of the space program, there have only been six missions to libration points, and all have been in the Sun-Earth system [Ref 1-2]. The first Lagrange or libration point mission was the International Sun-Earth Explorer-3 (ISSE-3) [Ref 3] launched in 1978. ISSE-3 maintained a complex orbit shown in Figure 4, about the L1 point to the Sun-Earth system, where it observed and detected solar flares and cosmic gamma ray bursts. The Halo orbit allowed the spacecraft to make observations over one and a half million kilometers closer to the Sun than ISEE-1 and ISEE-2, which were in Earth orbits, and demonstrated the advantage and flexibility of Halo orbit missions. While the two Earth based satellites re-entered atmosphere at end of life, ISSE-3 was renamed International Cometary Explorer and sent to rendezvous with the comet, Giacobini-Zinner and flew through its the tail in 1985.

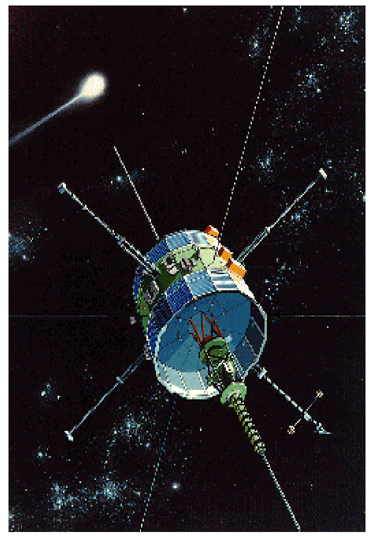

Figure 3. ISSE-3 Spacecraft [From: Ref 3]

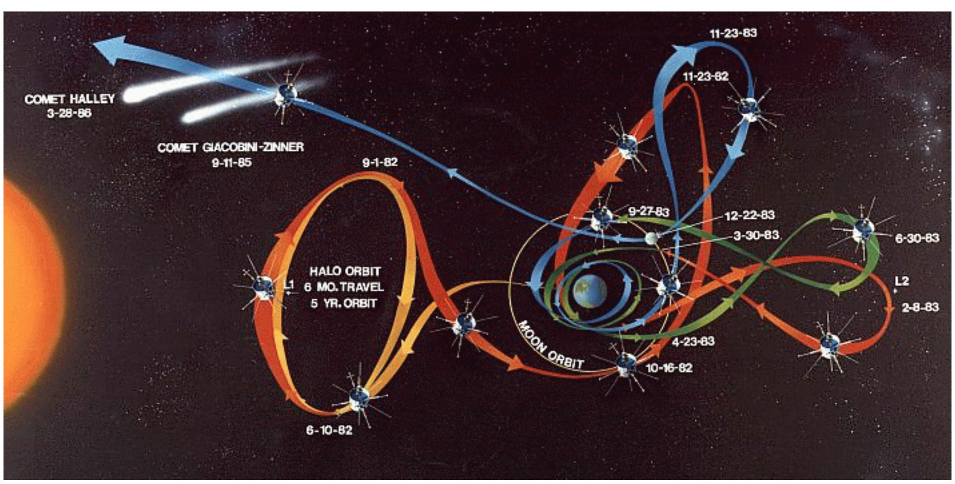

Figure 4. ISEE-3 Mission Trajectory [From: Ref 3]

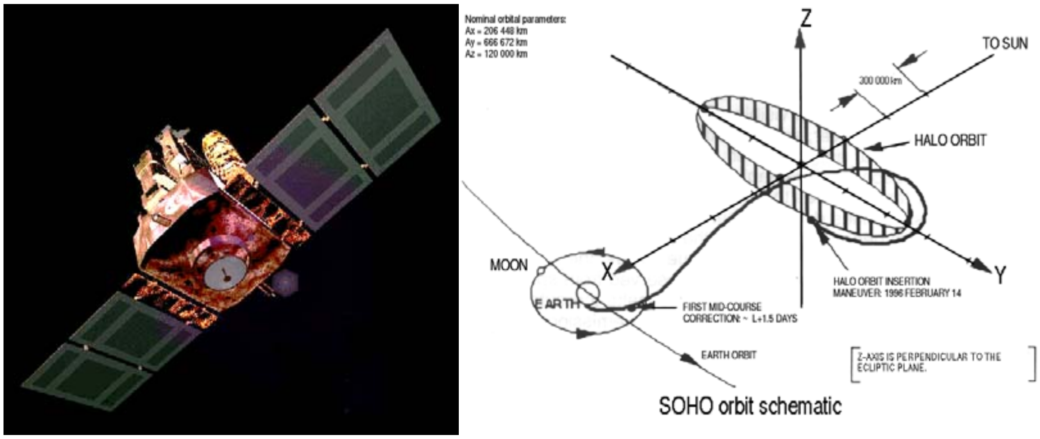

Figure 5. SOHO Satellite and Trajectory [From: Ref 4]

Perhaps the most famous Halo orbit mission is the Solar and Heliospheric Observatory (SOHO), which was launched in 1995 [Ref 4]. Like its predecessor ISSE-3, SOHO also orbits the L1 point of the Sun-Earth system and is dedicated to an intensive and continuous study of the star.

The most unique libration point mission to date has been WIND, which was launched in 1994 as part of the Global Geospace Science initiative [Ref 5]. WIND investigated and studied plasma, and magnetic field effects in both ionispheric and magnetospheric phenomena, and made baseline observations in the ecliptic plane for

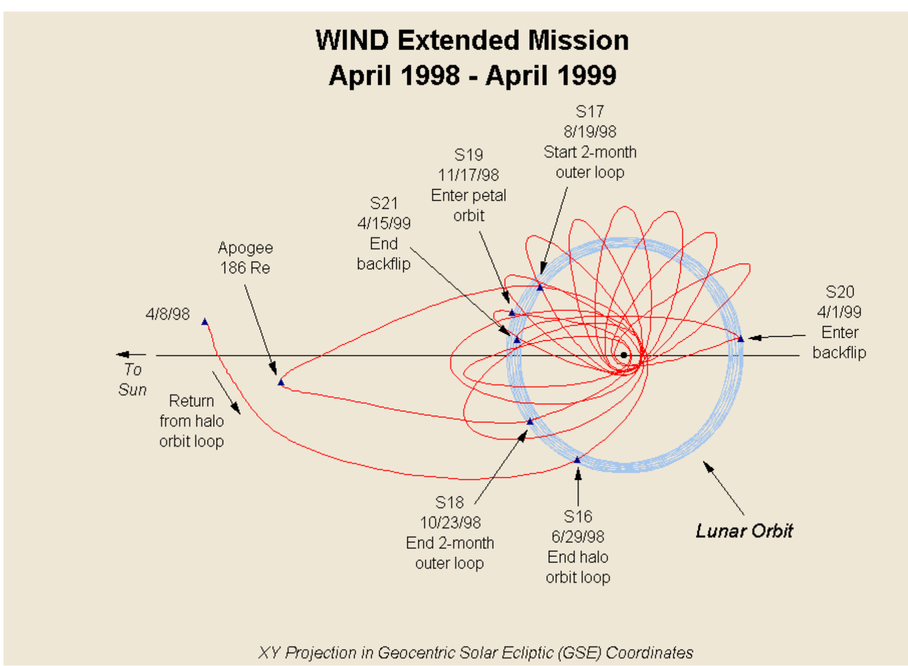

Figure 6. Extended WIND Mission Trajectory [From: Ref 5]

future missions. Its initial trajectory included multiple passes of the Moon before settling into a Halo orbit about the L1 point in the Sun-Earth System. Several months later it departed the L1 point for an additional lunar swing by before it initiated a series of petal orbits taking it out of the ecliptic.

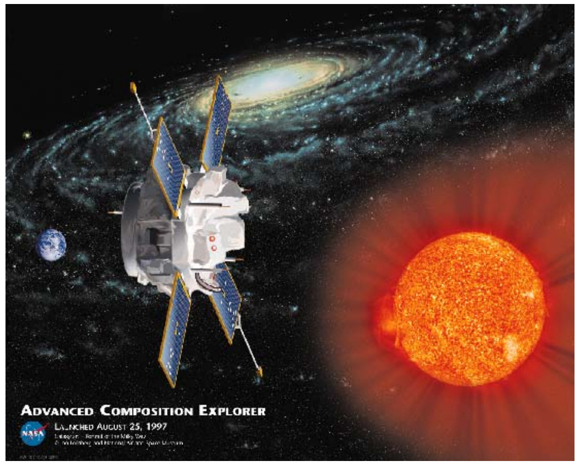

Figure 7. Advanced Composition Explorer (ACE) [From: Ref 6]

In the tradition of SOHO, the Advanced Composition Explorer (ACE), launched in 1997 [Ref 6], also orbits the Sun-Earth system L1 point, and obtains more specific and detailed measurements. The Microware Anisotropy Probe (MAP) was launched in 2001 and marked the first mission to the L2 point of the Sun-Earth System, where it looks deep in to space to decipher the age, geometry, and size of the universe without the obstructions of the Earth, Sun or Moon [Ref 7].

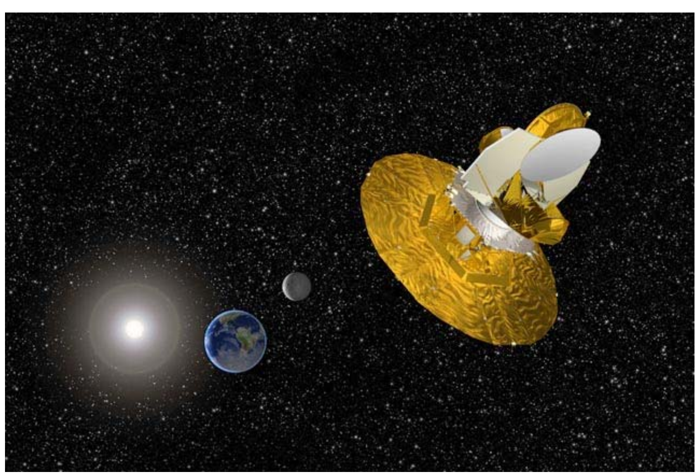

Figure 8. Microwave Anisotropy Probe (MAP) [From: Ref 7]

The most recent libration point mission is NASA's Genesis, which reached the L1 Sun-Earth point in 2001 using a Lissajous Orbit Insertion (LOI), which resembles a figure eight trajectory [Ref 8]. Genesis is collecting actual specimens of solar wind particles that it is then returning to Earth. Future Halo mission include Darwin, the Infrared Space Interferometry Mission [Ref 9], which like MAP will orbit the L2 Sun-Earth point in search of Earth-like planets using six telescopes. Darwin is not scheduled to launch until 2014.

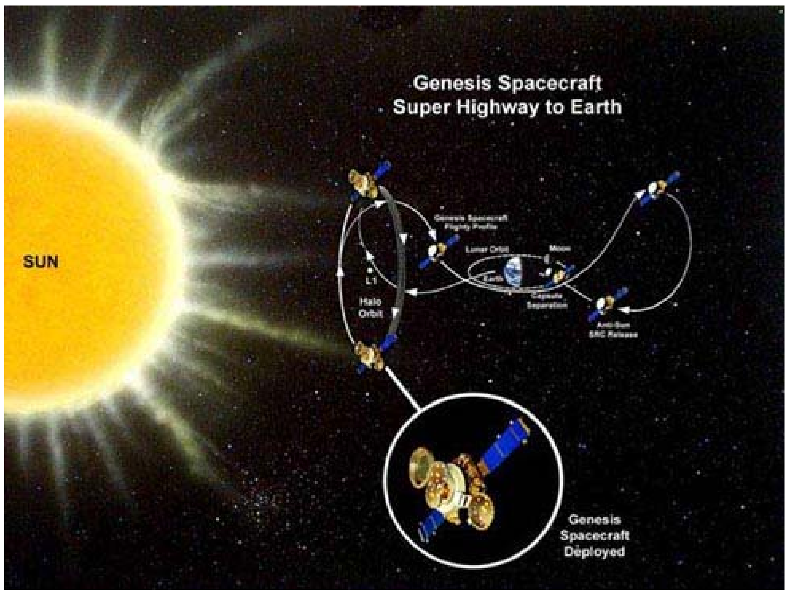

Figure 9. Genesis Lissajous Trajectory [From: Ref 8]

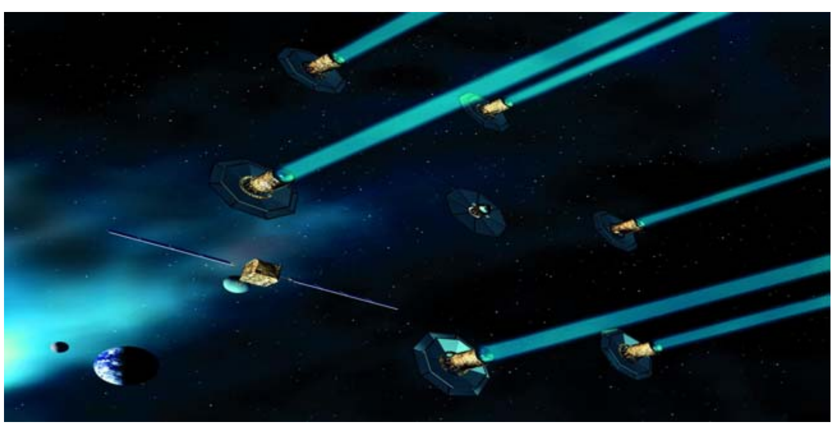
Figure 10. Darwin Telescope Flotilla [From: Ref 9]

III. HALO ORBIT PROBLEM FORMULATION

A. COORDINATE SYSTEM

1. Earth-Moon System

The geometry for the restricted three-body problem consists of two coordinate systems, the synodic and the barycentric [Ref 13-14]. The libration points in any three-body system exist in the rotating synodic (x_S, y_S, z_S) coordinate system. The barycentric frame is the inertial reference with respect to the Sun, and is fixed at the barycenter of the system. The subscript one identifies parameters associated with primary body; Earth, and the subscript two identifies parameters associated with the secondary body, which for this system is the Moon, shown below in Figure 10.

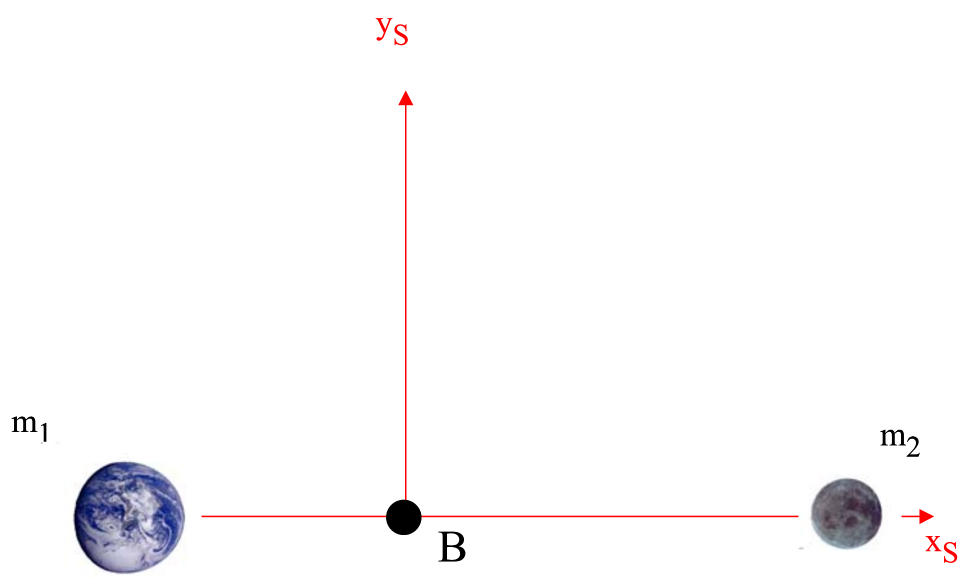

Figure 11. Earth-Moon System Geometry

2. Scaling

The variable and units in the problem are naturally non-dimensionalized. This problem is scaled using the variable μ^*, which should not be confused with the gravitational parameter, μ [Ref 13-14]. The location of the barycenter for the system is historically determined by the ratio μ^*, which is both the mass ratio $= \frac{m2}{m1+m2}$, and the ratio used to scale the distance between the primary and second body of the system by setting that distance = 1. For the Earth-Moon system specifically, $\mu^* = 0.0122$, where 1 distance unit (1 DU) is equal to the distance between the Earth and the moon; 384,400 km.

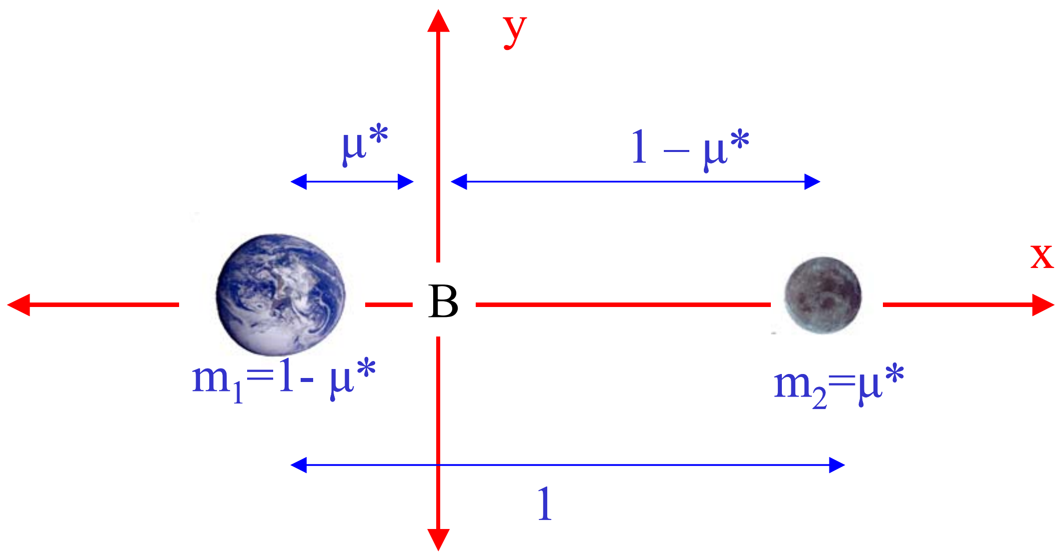

Figure 12. Mass and Distance Scaling for Earth-Moon System

	Mass		Distance from barycenter	
	kg	**scaled**	**km**	**scaled**
Earth	5.9742×10^{24}	0.9878	4690	0.0122
Moon	7.3483×10^{22}	0.0122	379,710	0.9878

Table 1. Mass and Distances for Earth-Moon System

3. Spacecraft Reference and Control

The controls of the spacecraft are simply defined by three thrust directions and are referenced to the synodic system (Tx, Ty, Tz) as shown on the following page in Figure 12. In this figure, the vector **R** is referenced from the origin, or the barycenter of the system. The spacecraft is also referenced from the primary (r_1) and secondary (r_2) bodies of the system for the purpose of formulating the spacecraft dynamics, which are shown in Figure 13 along with their derivation for use in the equations of motion. The thrust terms represent the control function of the spacecraft based on accelerations (a_x, a_y, a_z). Accelerations are used in the formulating the dynamics in order to simplify the problem without the need to select or consider specific propulsion ratings based on predicted mass flow rates and ISP performance.

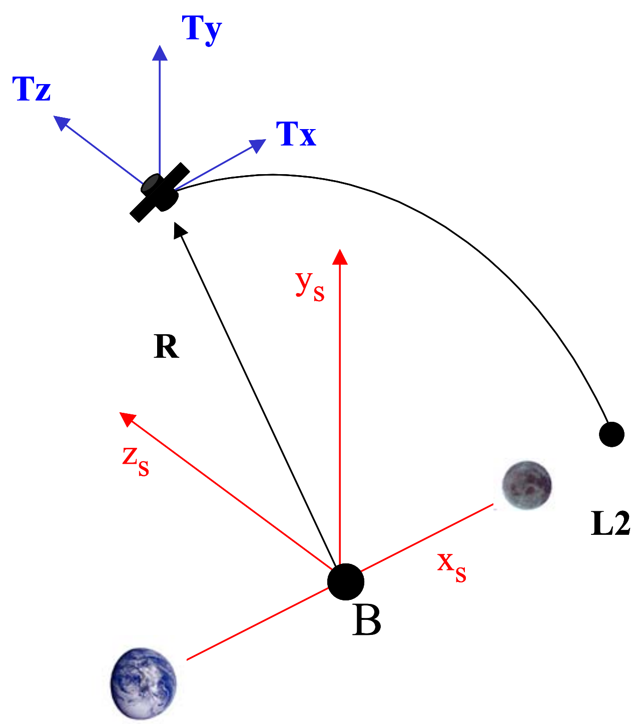

Figure 13. Spacecraft Reference

B. EQUATIONS OF MOTION

The following equations are the restricted three body equations of motion tailored to the problem [Refs 10,13-14], and modified to include an acceleration term (a_X, a_Y, a_Z) to represent the external force on the system, which is induced by the thrusting function of the spacecraft. The constant, μ^* is the mass ratio of the primary and secondary celestial bodies of the system and is defined as $\mu^* = 0.0122$, r_1 and r_2 are respectively referenced from the primary and secondary bodies of the system to the spacecraft;

$$\ddot{x} - 2\dot{y} - x = -\frac{(1-\mu^*)(x+\mu^*)}{r_1^3} - \frac{\mu^*(x-1+\mu^*)}{r_2^3} + a_X \qquad \text{eqn (1)}$$

$$\ddot{y} + 2\dot{x} - y = -\frac{(1-\mu^*)y}{r_1^3} - \frac{\mu^* y}{r_2^3} + a_Y \qquad \text{eqn (2)}$$

$$\ddot{z} = -\frac{(1-\mu^*)z}{r_1^3} - \frac{\mu^* z}{r_2^3} + a_Z \qquad \text{eqn (3)}$$

It is important to specify the spacecraft position vectors, r_1 and r_2, with respect to their reference body. These vectors are different and alter the dynamics of the problem depending on whether the spacecraft is in the positive or negative x quadrant of the coordinate system. This thesis focuses on solutions at the L2 and L4 libration points, whose locations for this problem are defined in the positive x quadrant. The definition of r_1 and r_2 is illustrated below in Figure 13 and in equations (4-5);

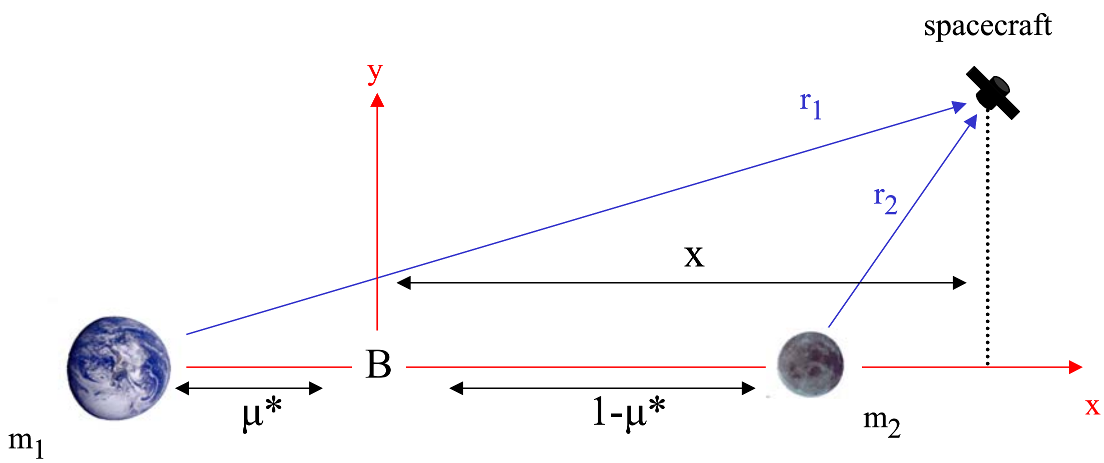

Figure 14. Defining r_1 and r_2

$$r_1 = \sqrt{(x+\mu)^2 + y^2 + z^2} \qquad \text{eqn (4)}$$

$$r_2 = \sqrt{(x-\mu+1)^2 + y^2 + z^2} \qquad \text{eqn (5)}$$

C. LIBRATION POINTS

The actual equilibrium points in the system are located in the rotating coordinate system by setting the out of plane velocity and acceleration to zero in the restricted three body equations of motion set [Refs 13-14]. The thrust or acceleration term is also dropped out in order to find the stationary libration points in the rotating frame.

$$x = \frac{(1-\mu^*)(x+\mu^*)}{r_1^3} + \frac{\mu^*(x-1+\mu^*)}{r_2^3} \qquad \text{eqn (6)}$$

$$y = \frac{(1-\mu^*)y}{r_1^3} + \frac{\mu^* y}{r_2^3} \qquad \text{eqn (7)}$$

$$0 = \frac{(1-\mu^*)z}{r_1^3} + \frac{\mu^* z}{r_2^3} \qquad \text{eqn (8)}$$

In order for eqn (8) to be satisfied, z must equal zero, therefore any equilibrium position in the Lagrange system must be in the same or orbital plane (xy) as the primary (m_1) and secondary mass (m_2). Eqn (7) can be further simplified below by setting y=0 in eqn (9).

$$0 = y(1 - \frac{(1-\mu^*)}{r_1^3} + \frac{\mu^*}{r_2^3}) \qquad \text{eqn (9)}$$

and then solving for three co-linear Lagrange points on the x axis (L1, L2, L3), which are the three real roots of eqn (10).

$$x - \frac{(1-\mu^*)(x+\mu^*)}{r_1^3} - \frac{\mu^*(x-1+\mu^*)}{r_2^3} = 0 \qquad \text{eqn (10)}$$

Substituting eqns (4) and (5) into eqn (10) and simplifying yields the following equation;

$$x - \frac{(1-\mu^*)}{(x+\mu^*)} + \frac{\mu^*}{(x-1+\mu^*)^2} = 0 \qquad \text{eqn (11)}$$

The solution to eqn (10) and the locations of the three co-linear libration points are obtained by first finding the three real roots to the Euler *quintic equations* [Ref 15] shown in eqn (12);

$$\begin{aligned}&(m_1+m_2)x^5+(3m_1+2m_2)x^4+(3m_1+m_2)x^3-(m_2+3m_3)x^2\\ &\quad-(2m_2+3m_3)x+(m_2+m_3)=0\end{aligned} \qquad \text{eqn (12)}$$

or as Vallado [Ref 14] expresses in three equations, eqns (13-15) where m_1 is the mass of the primary body, m_2 is the mass of the secondary body, and m_3 is the mass of the spacecraft, which is generally negligible in comparison.

$$x^5 + (3-\mu^*)x^4 + (3-2\mu^*)x^3 - \mu^* x^2 - 2\mu^* x - \mu^* = 0 \qquad \text{eqn (13)}$$

$$x^5 - (3-\mu^*)x^4 + (3-2\mu^*)x^3 - \mu^* x^2 + 2\mu^* x - \mu^* = 0 \qquad \text{eqn (14)}$$

$$x^5 + (2-\mu^*)x^4 + (1+2\mu^*)x^3 - (1-\mu^*)x^2 - 2(1-\mu^*)x - (1-\mu^*) = 0 \quad \text{eqn (15)}$$

Using a numerical solution method, and substituting the mass values for Earth as the primary body, and the moon as the secondary, the three real roots of eqn (12-15) are found to be; (0.8380, 1.1500, -1.0050) [Ref 14]. The specific normalized x coordinates of the libration points for the Earth-Moon system are then shown below;

L1= (0.8380, 0, 0) L2= (1.1500, 0, 0) L3= (-1.0050, 0, 0)

Equations (9) and (10) can also be used to find the L4 and L5 Lagrange points by setting $r_1 = r_2 = 1$. Lagrange found the general location of these stable points based on the geometry of equilateral triangles [Ref 13,14,15] formed by the primary and secondary bodies of the system as shown in Figure 14;

L4 = ($\mu - 1/2, \sqrt{3}/2, 0$) L5 = ($\mu - 1/2, -\sqrt{3}/2, 0$)

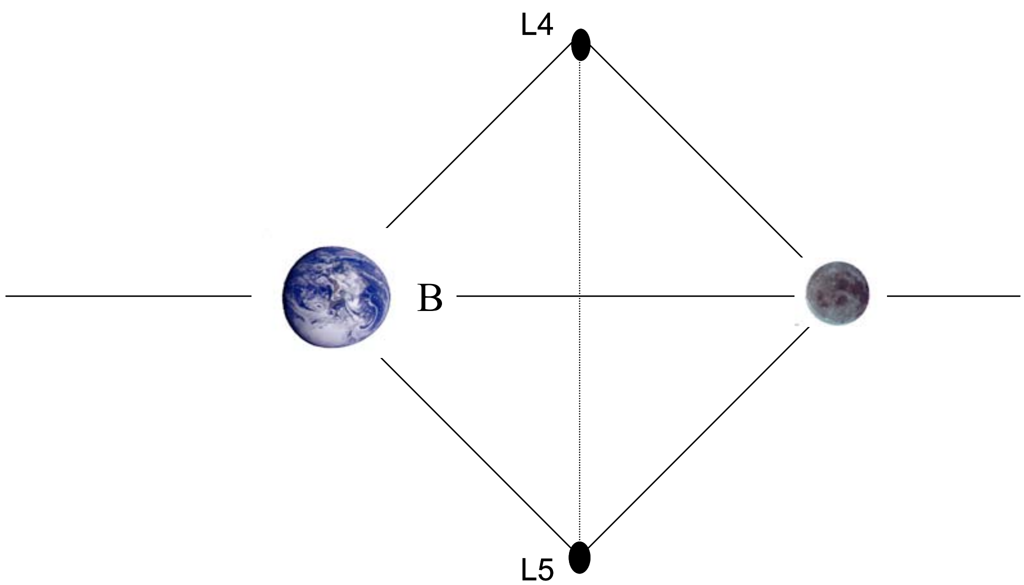

Figure 15. L4 and L5 Libration Point Geometry

For the Earth-Moon System theses coordinates are defined in scaled units as (0.4879, 0.8660, 0), and (0.4879, -0.8660, 0) respectively. Specific libration point locations for the Earth-Moon System in terms of scaled units and actual kilometers are summarized in Table 2 on the following page.

Point	X	Actual	Y	Actual	Z
	Scaled	**(km)**	**Scaled**	**(km)**	
Barycenter	0	0	0	0	0
L1	0.8380	322,120	0	0	0
L2	1.1500	442,060	0	0	0
L3	-1.0050	386,320	0	0	0
L4	0.4879	187,550	0.8660	332,890	0
L5	0.4879	187,550	-0.8660	-332,890	0

Table 2. Earth-Moon System Libration Point Numerical Coordinates

THIS PAGE INTENTIONALLY LEFT BLANK

IV. OPTIMAL CONTROL PROBLEM AND ORBIT DESIGN

The solution to any optimal control problem is generally attained by "solving for the state and control histories of a system subject to constraints while minimizing (or maximizing) some performance index." [Ref 17] DIDO is an optimization software package [Ref 18] that runs within an existing MATLAB program, it "employs a powerful direct Legendre pseudospectral method that exploits the sparsity pattern of the discrete Jacobian by way of the Nonlinear Programming solver SNOPT" [Ref 19]. After formulating a general problem, a user makes inputs using basic MATLAB functions and files according to the appropriate DIDO format. This format or setup primarily consists of basic optimizing building blocks including dynamics, constraints, events, bounds, and cost that make up various sub-files and are mapped back to the main solution file.

For simplicity, a dual approach was used to tackle this problem. First, an optimal solution of an orbit about the L4 libration point was sought, since this is a stable point where a solution is more easily obtained than an unstable point. Next, the problem was restructured to exploit the potential for trajectories about the unstable L2 libration point.

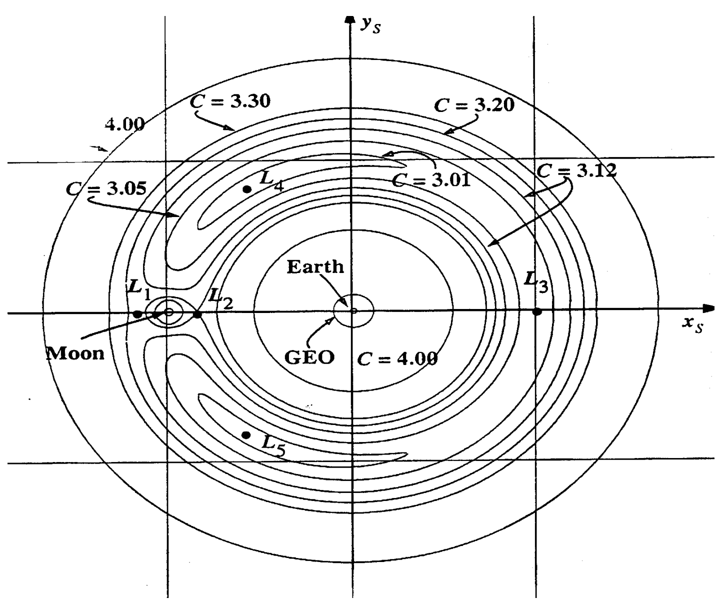

Figure 16. Regions of xy Motion for the Earth-Moon System [From: Ref 14]

Figure 16 illustrates the differences between the zero motion regions about the libration points of the Earth-Moon system in the x-y and x-z planes. In this figure, motion across curves (C) of lesser value may only be attained with additional thrust.

A. DYNAMICS

The restricted three body equations of motion (eqns 1-3) determine the dynamics of the problem. These dynamics reside in an exclusive sub-file that contains the equations of motion. In the dynamic constraint τ , is an independent variable, which is usually but not necessarily time [Ref 20].

$$\text{State vector x} = \begin{bmatrix} r_X \\ r_Y \\ r_Z \\ v_X \\ v_Y \\ v_Z \end{bmatrix} \qquad \text{Control vector u} = \begin{bmatrix} a_X \\ a_Y \\ a_Z \end{bmatrix} \qquad \begin{bmatrix} r_X \\ r_Y \\ r_Z \\ v_X \\ v_Y \\ v_Z \\ a_X \\ a_Y \\ a_Z \end{bmatrix} = \begin{bmatrix} x \\ y \\ x \\ \dot{x} \\ \dot{y} \\ \dot{z} \\ \ddot{x} \\ \ddot{y} \\ \ddot{z} \end{bmatrix}$$

$$\dot{x}(\tau) = f(x(\tau), u(\tau), \tau) \qquad \text{eqn (16)}$$

B. EVENT CONDITIONS

The event conditions for the problem are established by assigning values to the initial (0) and final (F) values of the states or boundary conditions. For this problem, it was not necessary to assign any particular value to these events. Instead, it was important that the initial and final events equal each other, meaning that the final position of the spacecraft match it's starting position in order to signify a completed orbit.

$r_{X0} - r_{XF} = 0 \qquad v_{X0} - v_{XF} = 0$

$r_{Y0} - r_{YF} = 0 \qquad v_{Y0} - v_{YF} = 0$

$r_{Z0} - r_{ZF} = 0 \qquad v_{Z0} - v_{ZF} = 0$

In order to ensure the initial and final conditions are equal, the value of each event condition is set to zero in the main file by setting the both the upper and lower bounds of the event conditions to zero.

C. GUESSES

Initial guesses are required for the initial and final conditions of the states, controls, and time in the DIDO problem formulation. The guess does not necessarily need to be feasible, and can be a simple estimate or prediction. However, in the unstable libration point solutions, a reasonable guess was essential because of its extreme sensitivity. In this case, where the user may not be confident in the reasonability of the guess, a "bootstrapping" technique may be used and is applied to this problem. In this process an initial iteration is run using a small number of nodes. This initial run may output a crude or sub-optimal solution, but is usually more reasonable than the guess. This output is fed back through the optimization process again, where this initial solution is used as the guess for the second iteration. The initial guesses for this problem are scaled and defined in Table 3 below. Guesses for time were based on π and 2π, which are typical periods for halo orbits [Ref 10,12].

Guesses								
	Stable Solution				Unstable Solution			
	Initial Iteration		Second Iteration		Initial Iteration		Second Iteration	
States	Initial	Final	Initial	Final	Initial	Final	Initial	Final
r_X	0.4879	0.4879	0.4883	0.4883	1.1500	1.1500	1.0505	1.0505
r_Y	0.8660	0.8660	0.8659	0.8659	0	0	-0.1465	-0.1465
r_Z	0	0	-0.0018	-0.0018	0	0	0.0000	0.0000
v_X	0	0	0.0003	0.0003	0	0	-0.0191	-0.0191
v_Y	0	0	0.0001	0.0001	0	0	0.1889	0.1889
v_Z	0	0	0	0	0	0	0.0000	0.0000
Controls								
a_X	0	0	0.0063	0.0059	0	0	0.0002	-0.0006
a_Y	0	0	0.0063	0.0060	0	0	0.0002	0.0022
a_Z	0	0	0.0058	0.0058	0	0	0.0006	0.0006
Time	0	6.2832	0	6.2832	0	3.1416	0	3.6637

Table 3. Guesses for Optimal Solution

D. BOUNDARY CONSTRAINTS

The events, states, controls of the problem are all assigned lower and upper bounds in the main program file in order to specifically define the problem and ensure feasible solutions are achieved. As discussed in Section B, the equations defined under the event conditions were set to equal zero such that there was no difference between the initial and final conditions. All values of the states, and controls, in which the DIDO optimization software could explore for a solution were constrained, so that the scope of the problem was restricted within the vicinity of the desired solution. These constraints were chosen to ensure that the output was in fact an orbit about the appropriate libration point, and did not allow the spacecraft to venture towards an orbit of the Earth, Moon, or another libration point by performing an unnecessary thrusting maneuver. An example of an improperly bounded problem is shown in Figure 15 below, where the solution seeks a

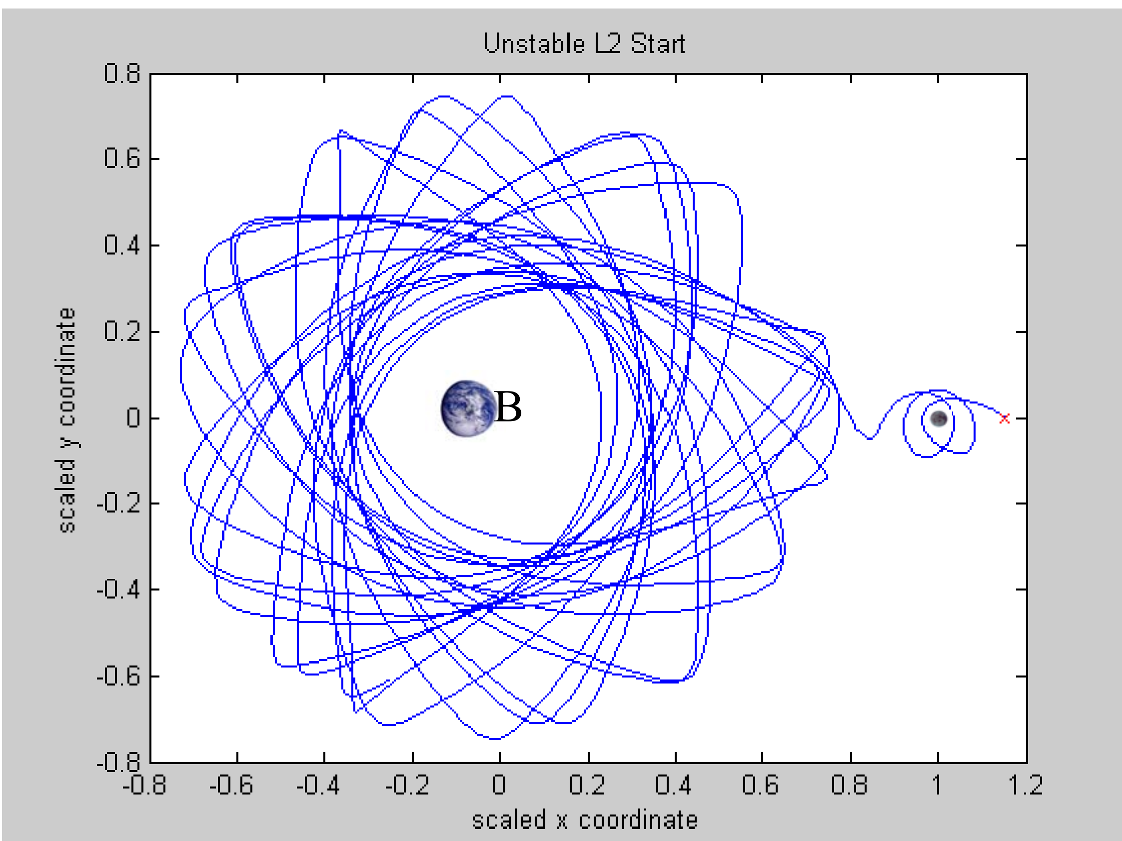

Figure 17. Unbounded Trajectory

trajectory about the Earth and system barycenter (B) after orbiting the moon although it began at the unstable L2 libration point. Though not optimized, this trajectory might prove useful in obtaining a solution for a low thrust transfer trajectory from Earth to a Halo orbit insertion orbit about the L2 libration point of the Earth-Moon system and has been previously presented in [Ref 11] and is shown below in Figure 18.

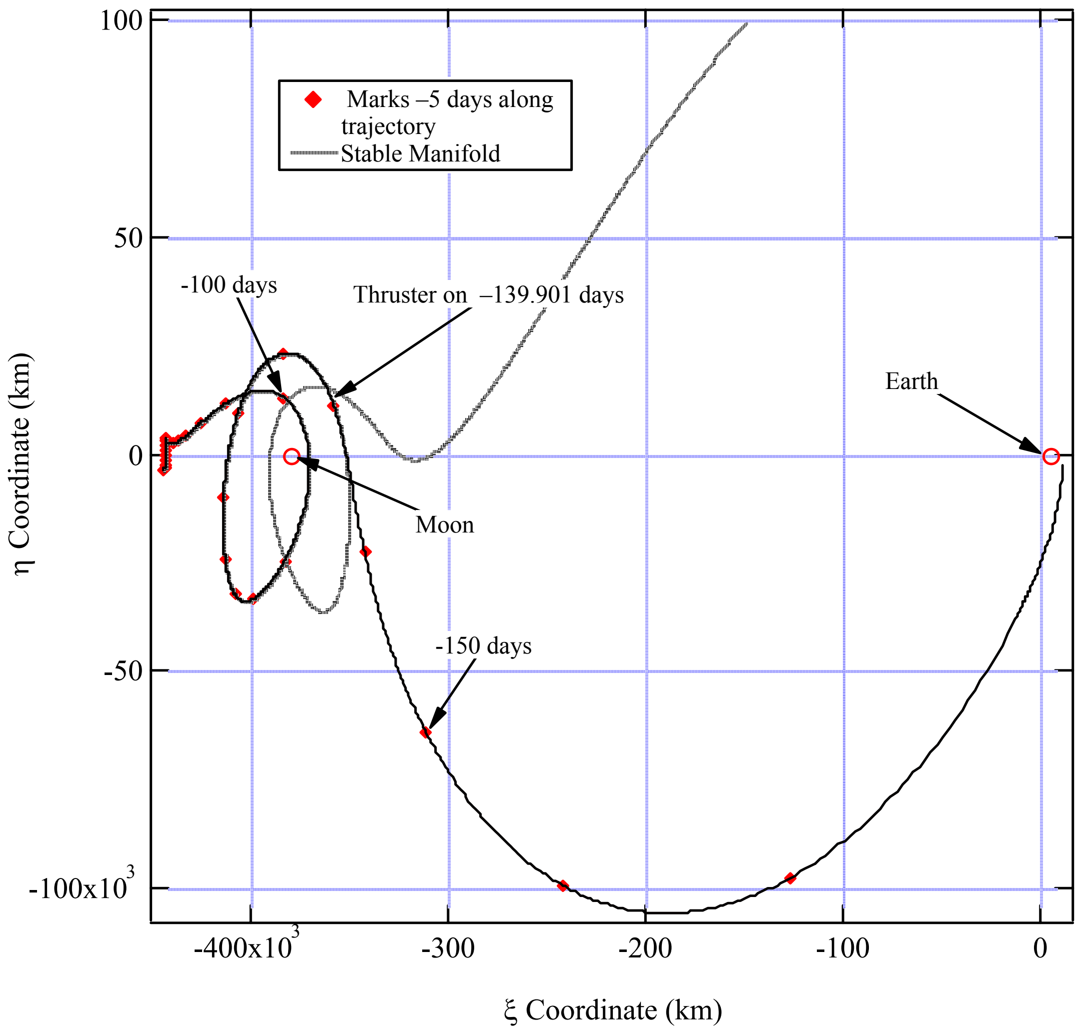

Figure 18. Libration Point Orbit Insertion [From: Ref 11]

Constraints on the events, states, and controls are expressed in eqns (17-19) [Ref 20] respectively, and all upper and lower level bounds, including time, are scaled and listed in Tables 4 and 5 on the following page.

$$e_l \le e(x(\tau_0), x(\tau_f), \tau_0, \tau_f) \le e_u \qquad \text{eqn (17)}$$

$$x_l \le x(\tau) \le x_u \qquad \text{eqn (18)}$$

$$u_l \le u(\tau) \le u_u \qquad \text{eqn (19)}$$

Bounds for Time and Controls		
Time	Lower	Upper
	0	10000
Control	Lower	Upper
a_X	-5.0	5.0
a_Y	-5.0	5.0
a_Z	-5.0	5.0

Table 4. Time and Control Bounds

Bounds for States and Events								
	Stable Solution		Unstable Solution		Stable and Unstable Solution			
States	Lower	Upper	Lower	Upper	Events	Lower	Upper	
r_X	0.7	1.1	1.0	1.5	r_{X0} - r_{XF}	0	0	
r_Y	0.3	0.7	-0.5	0.5	$r_{Y0} - r_{YF}$	0	0	
r_Z	-0.5	0.5	-0.5	0.5	$r_{Z0} - r_{ZF}$	0	0	
v_X	-10	10	-10	10	r_{X0} - r_{XF}	0	0	
v_Y	-10	10	-10	10	$r_{Y0} - r_{YF}$	0	0	
v_Z	-10	10	-10	10	$r_{Z0} - r_{ZF}$	0	0	

Table 5. State and Event Bounds

E. NODES

The nodes represent markers or discrete points that define the states and controls throughout the problem. In general, using a higher number of nodes produces a more accurate solution and takes longer computational time. Initially, a lower number of nodes (approximately 100) was used for the crude preliminary solution and was fed into the following iteration via the bootstrap technique. For the seconds iteration a higher number of nodes was used (approximately 200) since the guess was more accurate, and therefore led to a more smooth and precise solution. As the problem was further explored and refined a higher number of nodes was used for the initial and bootstrapped solution respectively, which was actually applied to for both the stable and unstable solutions.

F. KNOTS

Knots are used in DIDO as a part of the optimization process and are used where there exists a potential for discontinuities in the intermediaries of the problem and typically at the end point conditions. In order to satisfy the solution format, the location, definition, upper and lower bounds must all be identified. The number of nodes used in obtaining a solution is also defined in terms of these knots. For this problem, knot locations were assigned to the initial and final values of time (t_0, t_F) and were defined as 'hard.' Upper and lower knot bounds were also defined for t_0 and t_F. The value of the node knot number was set to the corresponding number of nodes for both the initial and bootstrap solution, as discussed in the previous section.

G. COST

The key performance parameter by which the solution is measured is prioritized by the cost function. The minimization of a particular performance index is given in the form of the Bolza cost function,

$$J[x(\cdot),u(\cdot),\tau_0,\tau_f] = E(x(\tau_0),x(\tau_f),\tau_0,\tau_f) + \int_{\tau_0}^{\tau_f} F(x(\tau),u(\tau),\tau),d\tau \qquad \text{eqn (20)}$$

where E is the end point cost, and evaluates the cost function at boundary times and F is the integral cost and is evaluated over the time history of the function [Ref 20]. Ultimately this function is selected by the preference of the user, but two typical indices of optimality are minimum fuel and minimum time.

Conserving or minimize fuel expenditures is nominally a standard priority for any space mission. This is accomplished by minimizing control functions and thrust requirements within the propulsion budget of a spacecraft. In order to get x independent of the propulsion system, the following quadratic cost is used. It is important to note that there are multiple solutions of optimality to a problem, and that true optimality is only defined by the preference of the user or customer.

$$J = \frac{1}{(t_f - t_0)} \int_{\tau_0}^{\tau_f} (a_x^{\,2} + a_y^{\,2} + a_z^{\,2}) d\tau \qquad \text{eqn (21)}$$

H. PATH CONSTRAINT

In some optimization problems it is necessary to impose a mixed state control in seeking a solution. However, a path constraint was not required for this problem and was therefore left unspecified.

V. STABLE HALO ORBIT RESULTS

A. STABLE L4 SOLUTION

Due to the complexity of obtaining the solution for the unstable Lagrange points (L1, L2, L3), an orbit solution set was first found for a stable Lagrange point, specifically, L4. The initial solutions were propagated without a control function in order to verify Keplerian behavior, and are shown in following figures. Figures 19 and 20 represent the stable orbit solutions at L4 with no control functions and state boundaries imposed. These orbits are propagated out over a period of 100 consecutive periods and it demonstrates how the orbit expands. Figure 21 shows a bounded solution with no control propagated for approximately ten revolutions.

1. Zero Control Solutions

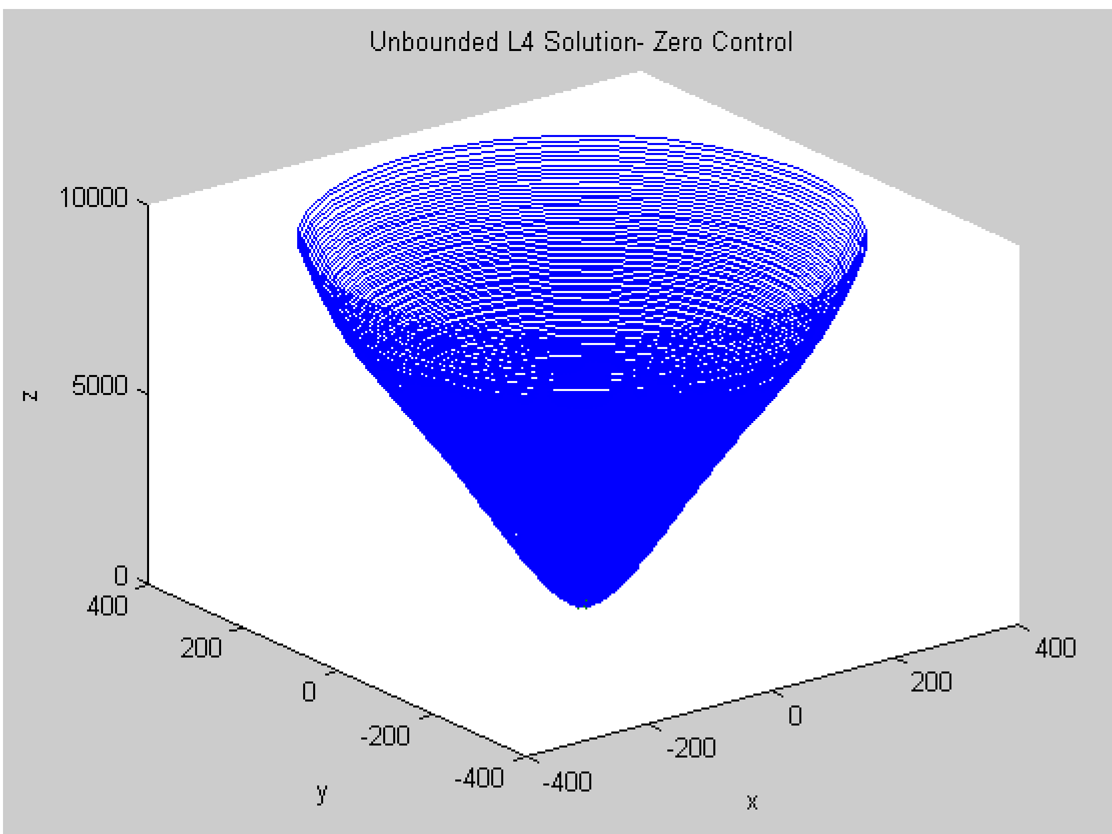

Figure 19. Unbounded 3D Solution– Zero Control

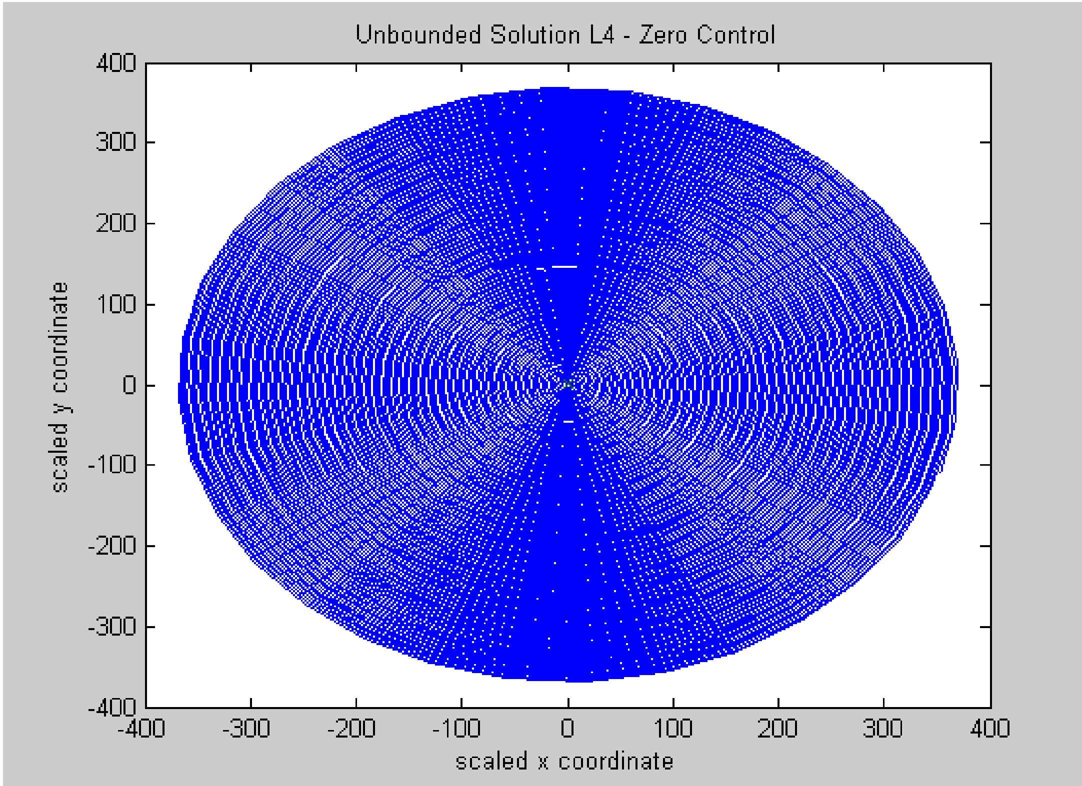

Figure 20. Unbounded 2D (xy plane) Solution– Zero Control

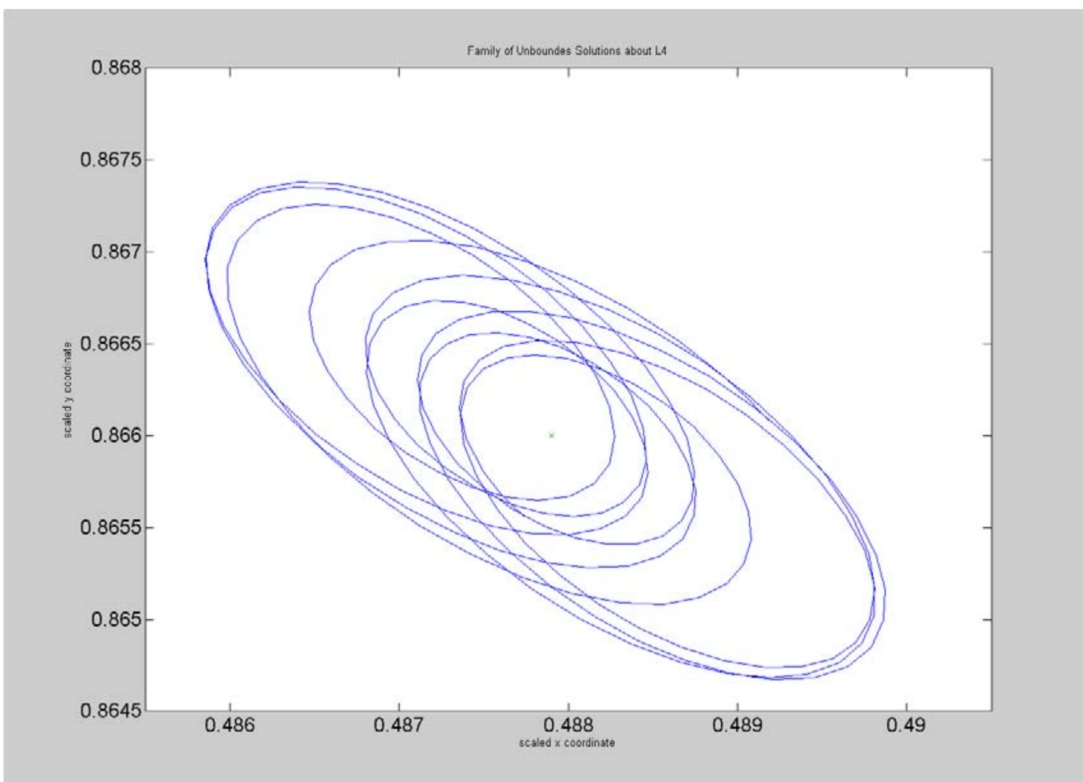

Figure 21. Family of Orbits for Bounded Solution – Zero Control

2. Controlled Solution

The solution for the constrained and controlled orbit about the stable L4 libration point is shown below in Figure 22 in the xy plane, and again in Figure 26 with respect to the Moon. The orbit is also shown relative to the position of the moon in the last figure of this section. These solutions were obtained using the quadratic cost function, and were locally optimal.

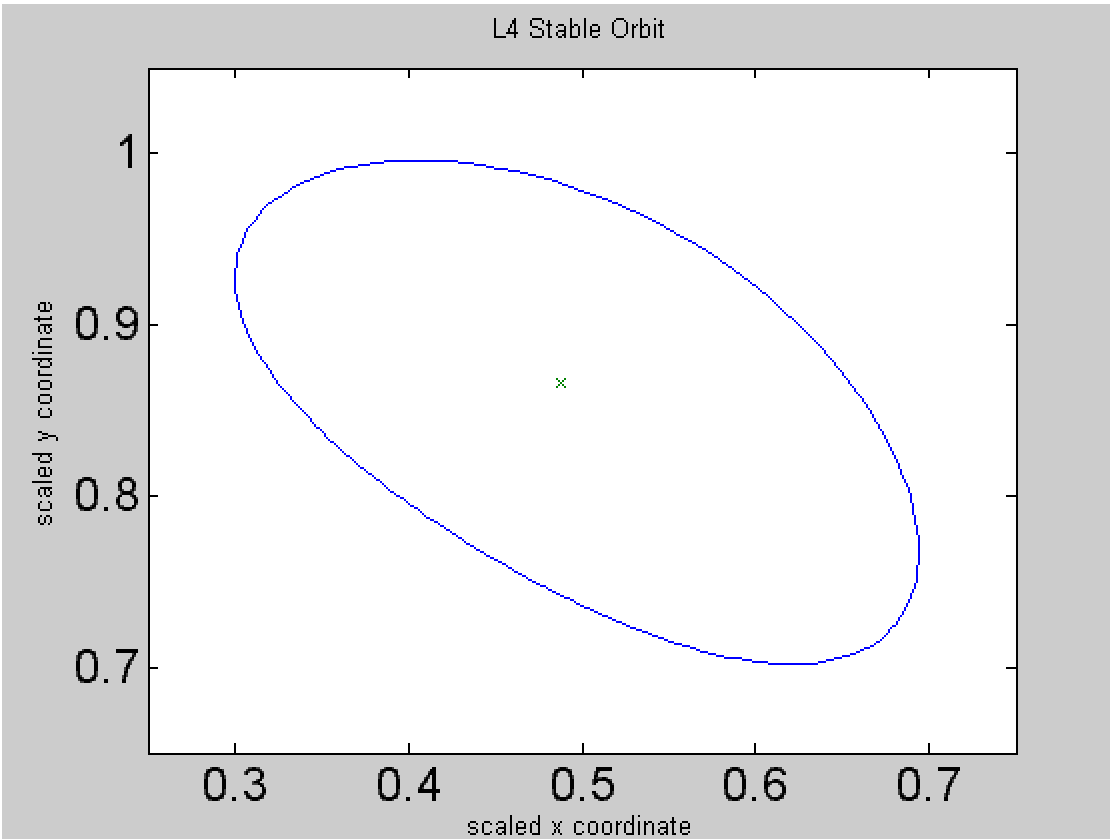

Figure 22. Stable L4 Libration Point Orbit in the xy Plane

The plots on the following pages include the state profiles in x-y-z, the respective velocities, and control functions for this particular solution all plotted against the normalized time, which were the nodes. For this solution set, one orbit corresponds to approximately 2π, and each plot reflects the periodicity of this time scale. It should be noted that the profiles in the z coordinate appear erratic, due to their scale, which is several orders of magnitude lower than the x, and y coordinates.

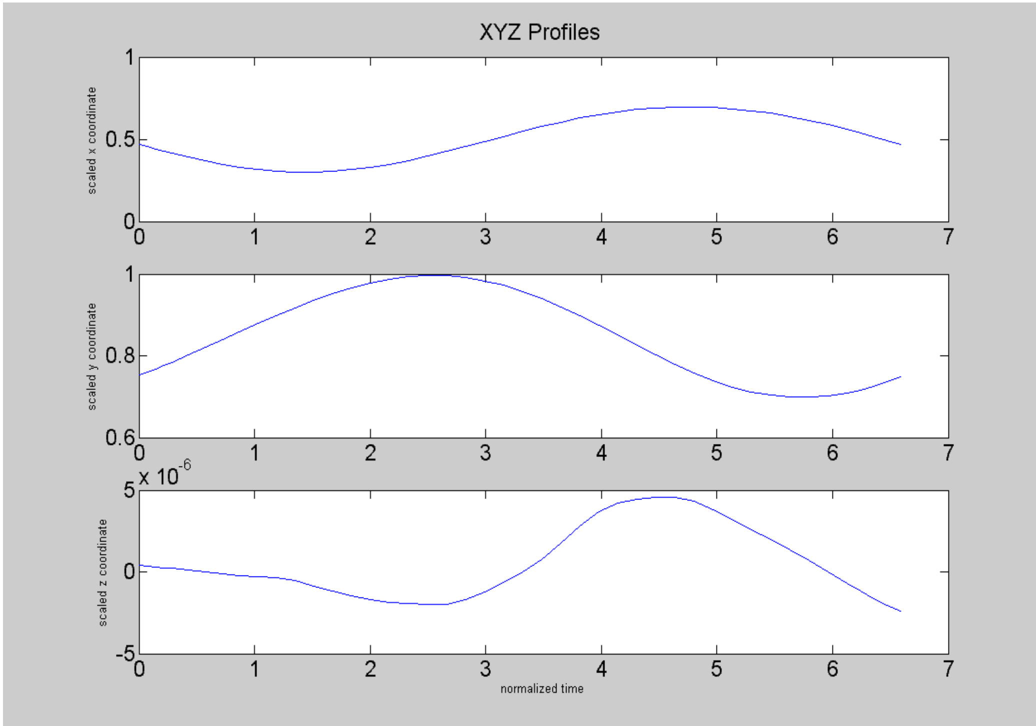

Figure 23. XYZ Profiles

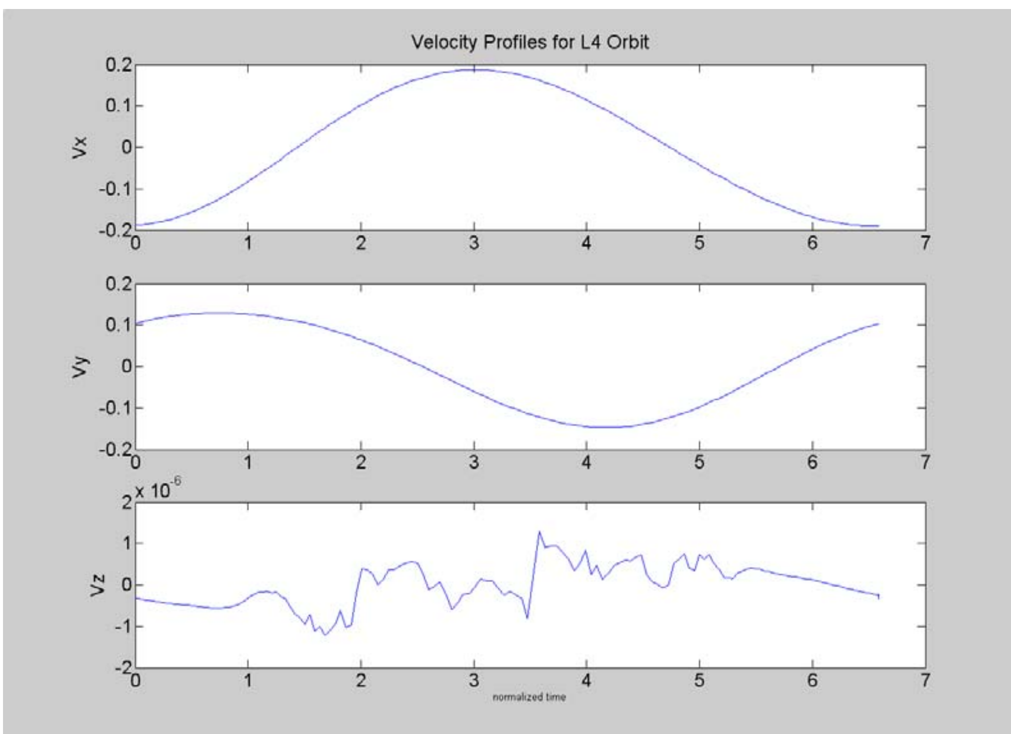

Figure 24. Velocity Profiles in XYZ

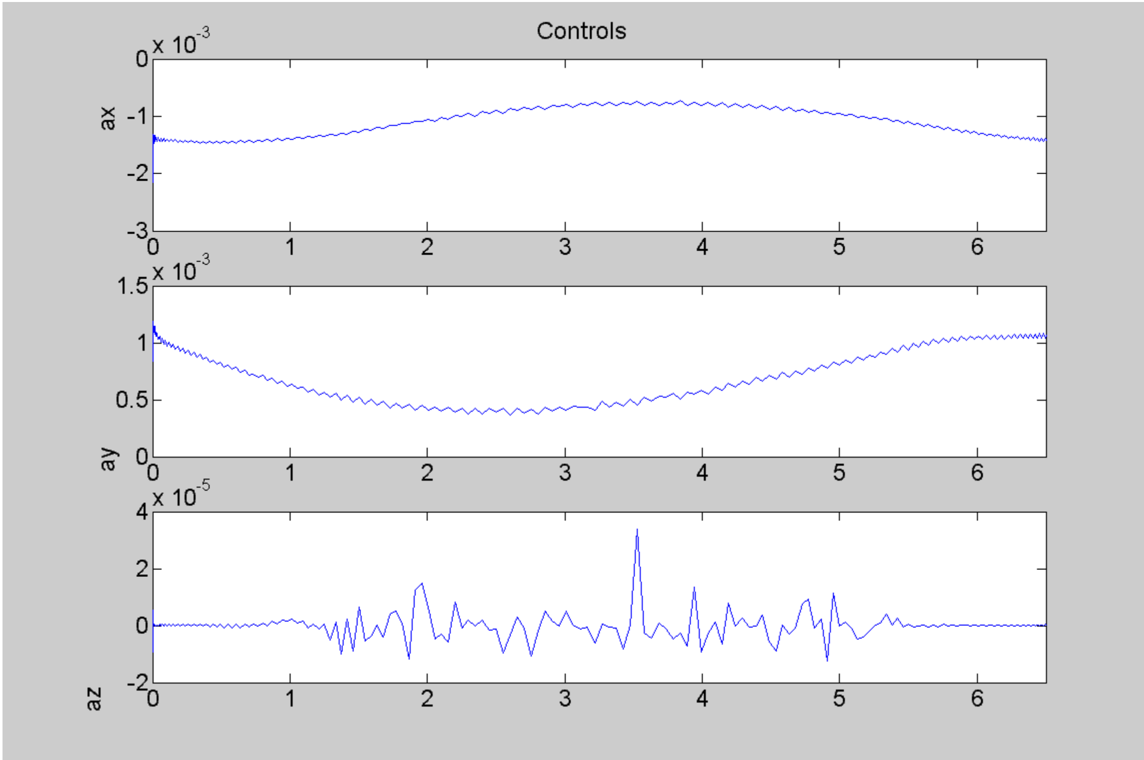

Figure 25. Controls

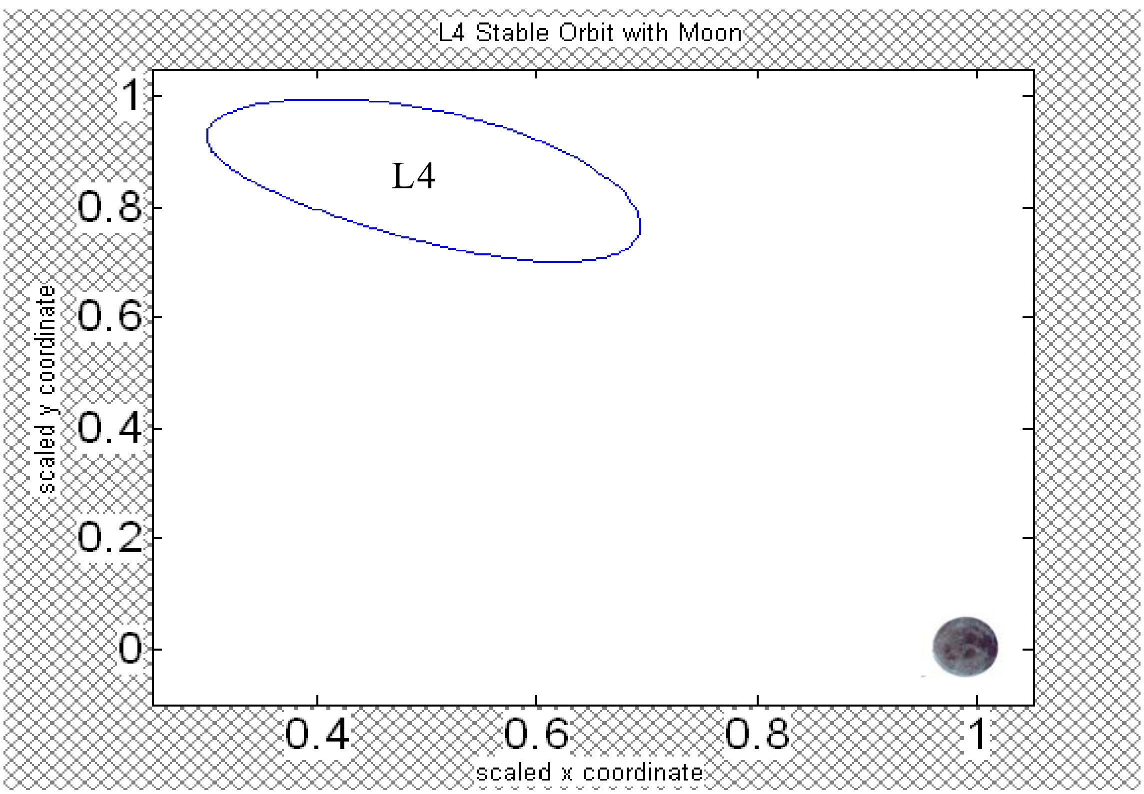

Figure 26. Stable L4 point orbit with Respect to Moon

B. VALIDATION

In order to verify the feasibility of the solution, the control solution generated by the DIDO optimizer is propagated through an ordinary differential equation solver using the same restricted three body equations of motion. The MATLAB function ODE 45, with the linear interpolation of the controls was used in this case. Figure 27 shows the comparison between the propagator solution shown in red and the DIDO trajectories in blue. Numerically, this difference in variation between the solutions is on the order of zero to 1.1 kilometers.

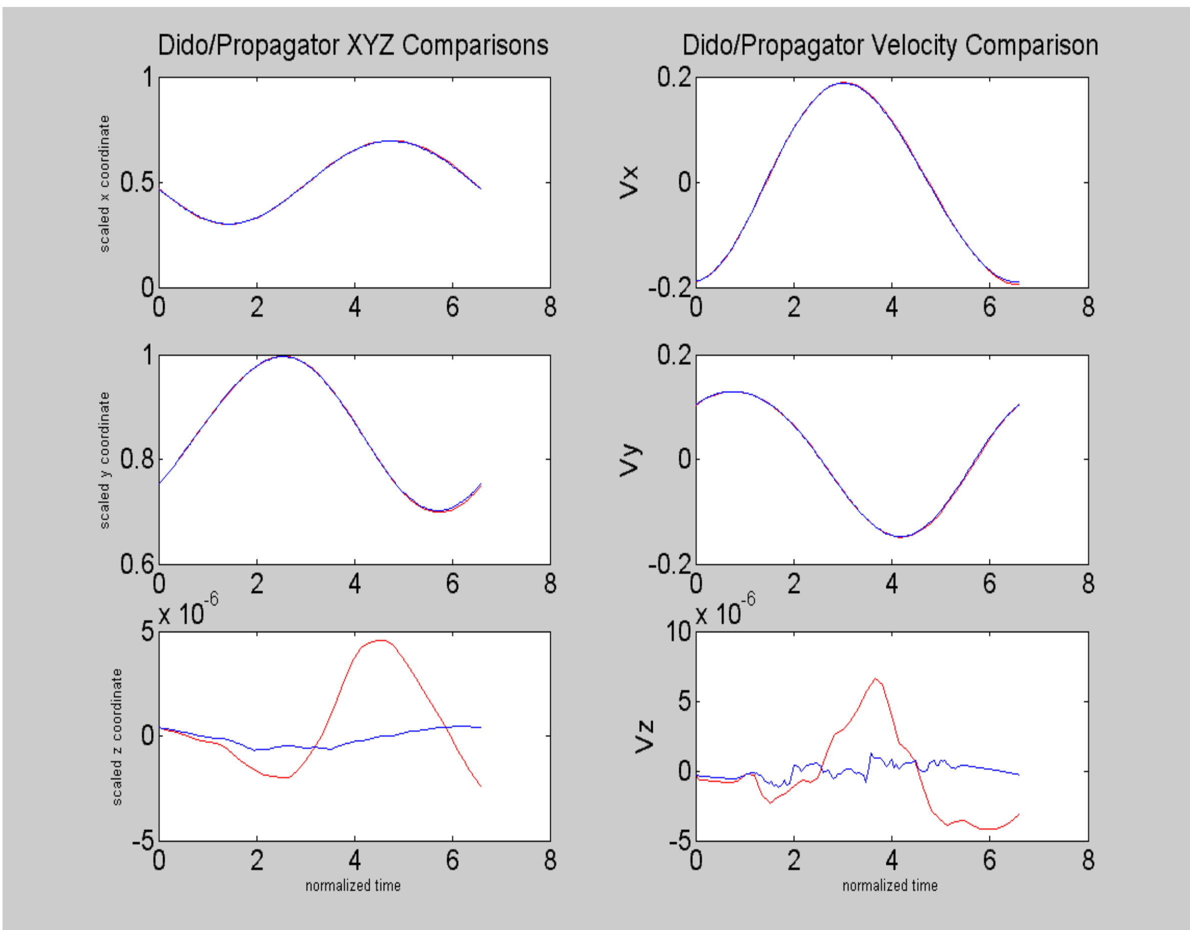

Figure 27. Propagator Comparisons

For this problem, it can be shown that the Hamiltonian plot is flat and near zero. The general Hamiltonian expression is shown in eqn (23) below followed by the Hamiltonian plot for this specific solution. In eqn (22) λ represents the Lagrange multipliers or costates, which are internal to the DIDO optimization solution [Ref 20].

$$H(x,u,\lambda,\tau) = F(x(\tau),u(\tau),\tau) + \lambda^T \bullet f(x(\tau),u(\tau),\tau) \qquad \text{eqn(22)}$$

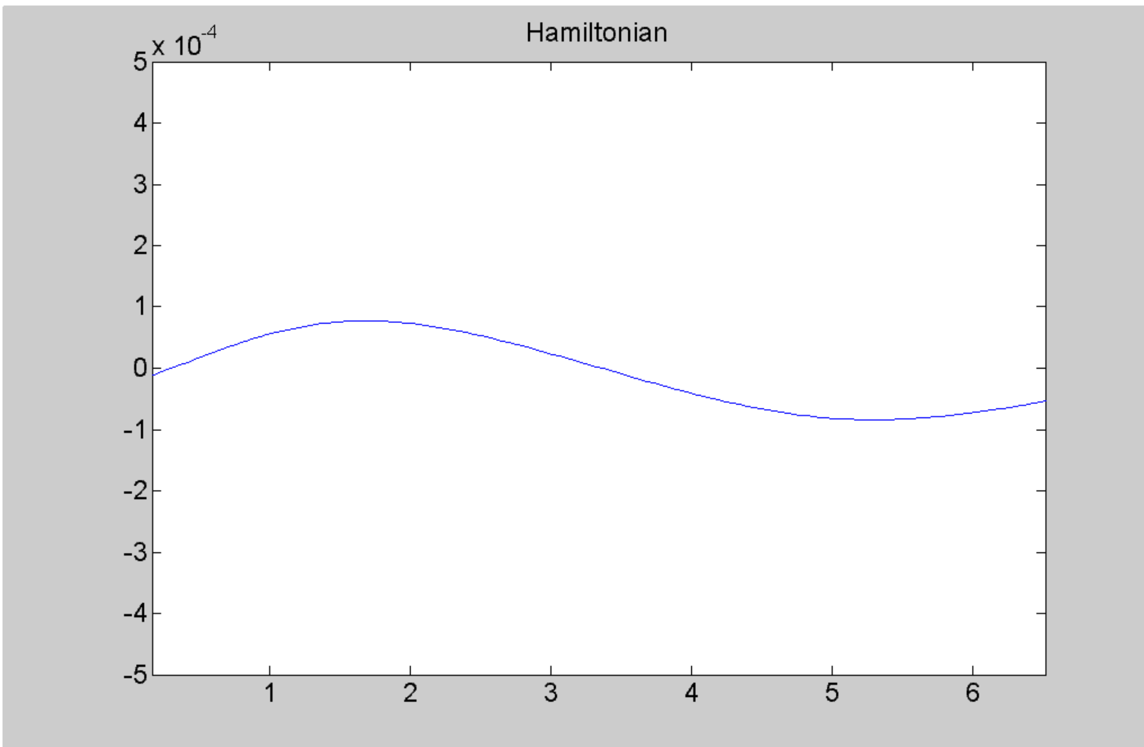

Figure 28. Hamiltonian for Stable L4 Libration Point Orbit Solution

THIS PAGE INTENTIONALLY LEFT BLANK

VI. UNSTABLE HALO ORBIT RESULTS

A. UNSTABLE L2 SOLUTION

Once the stable solutions were attained, the orbits for the unstable points were tackled with greater ease and some success. Because of the difference in location and stability, the L2 solution required different boundary conditions and guesses, but similar constraints. These values were presented with the orbit design in Section IV along with the stable solution values. As mentioned before, a reasonable guess for this solution was necessary in order to achieve feasible results. Unlike the stable orbit, it was even necessary to change the structure of the guess to resemble an orbit in the form of a circle for a feasible unstable solution. Making a circular guess about the unstable point, L2, encouraged a similar solution about the libration point. All solutions for the unstable points were found to be locally optimal and had a period that corresponded to π. Solutions in the similar format presented in Section V are shown below;

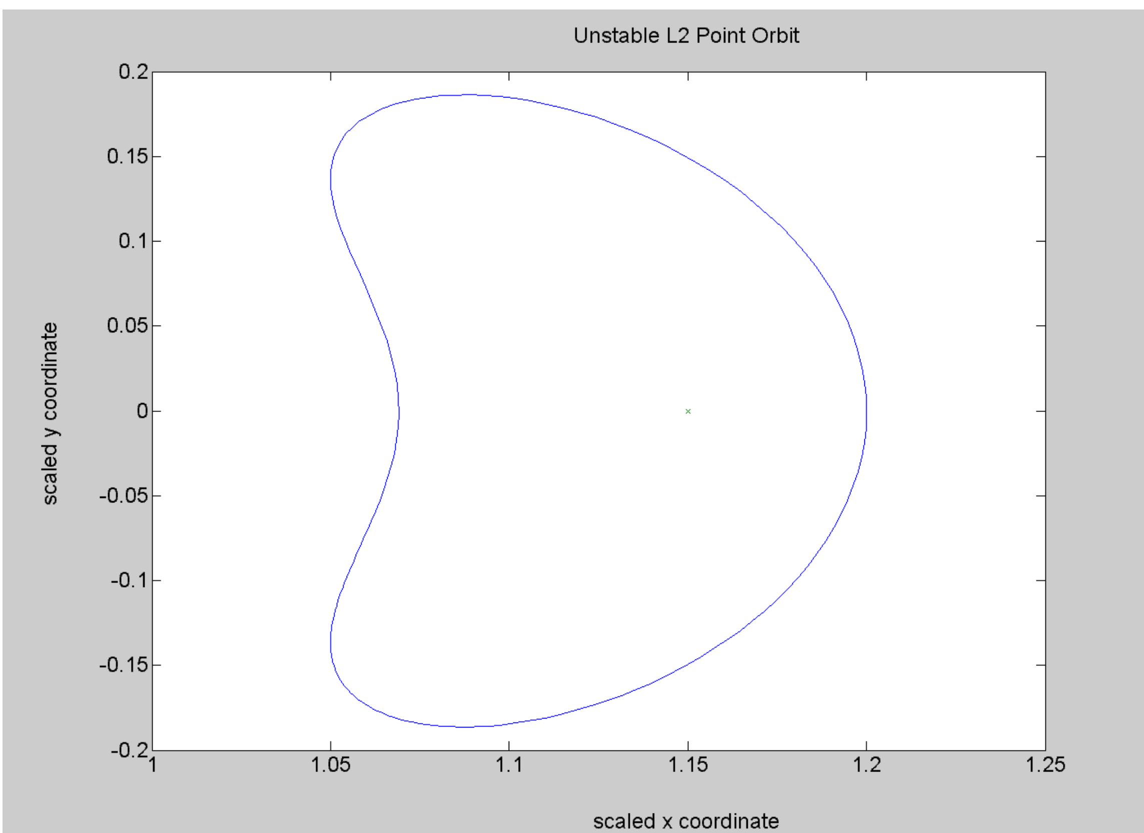

Figure 29. Unstable L2 Libration Point Orbit in the XY plane

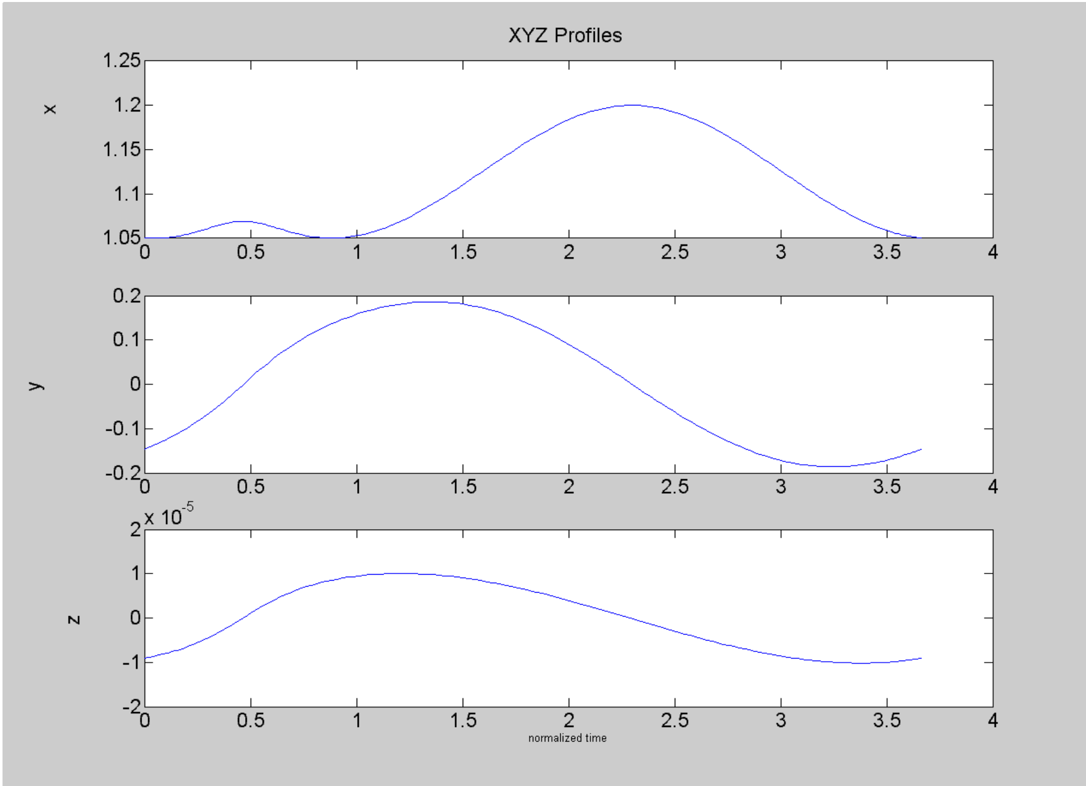

Figure 30. XYZ Profiles

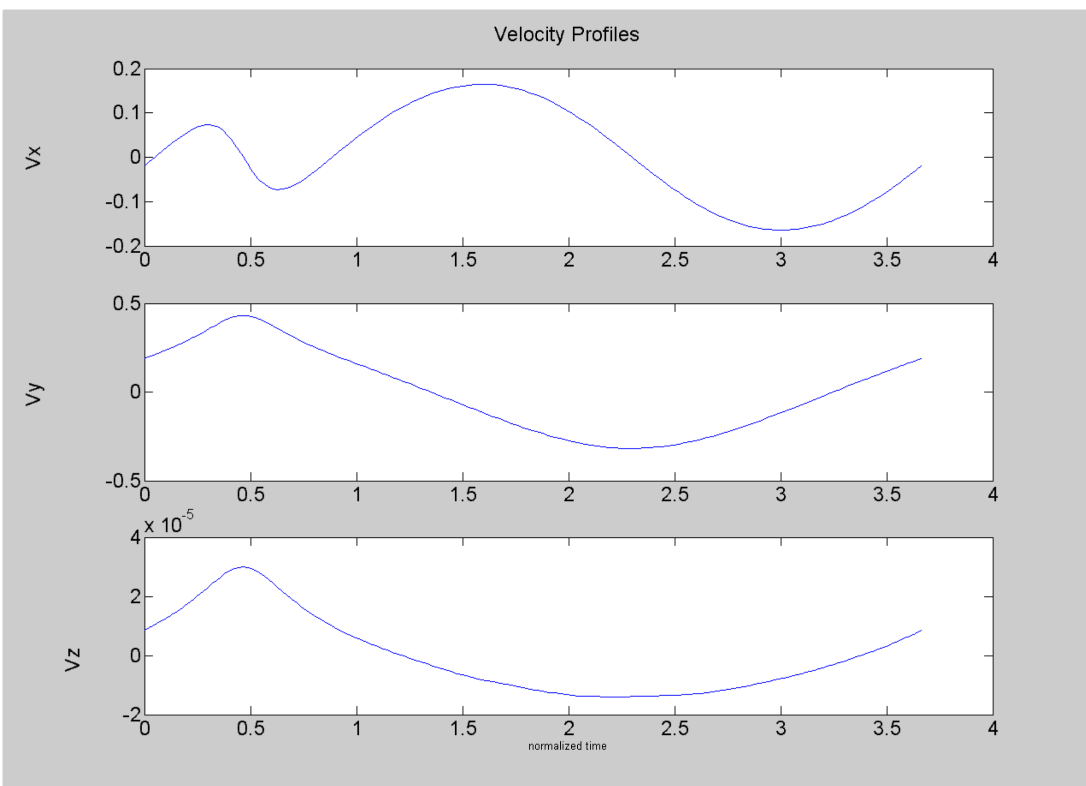

Figure 31. XYZ Velocity Profile

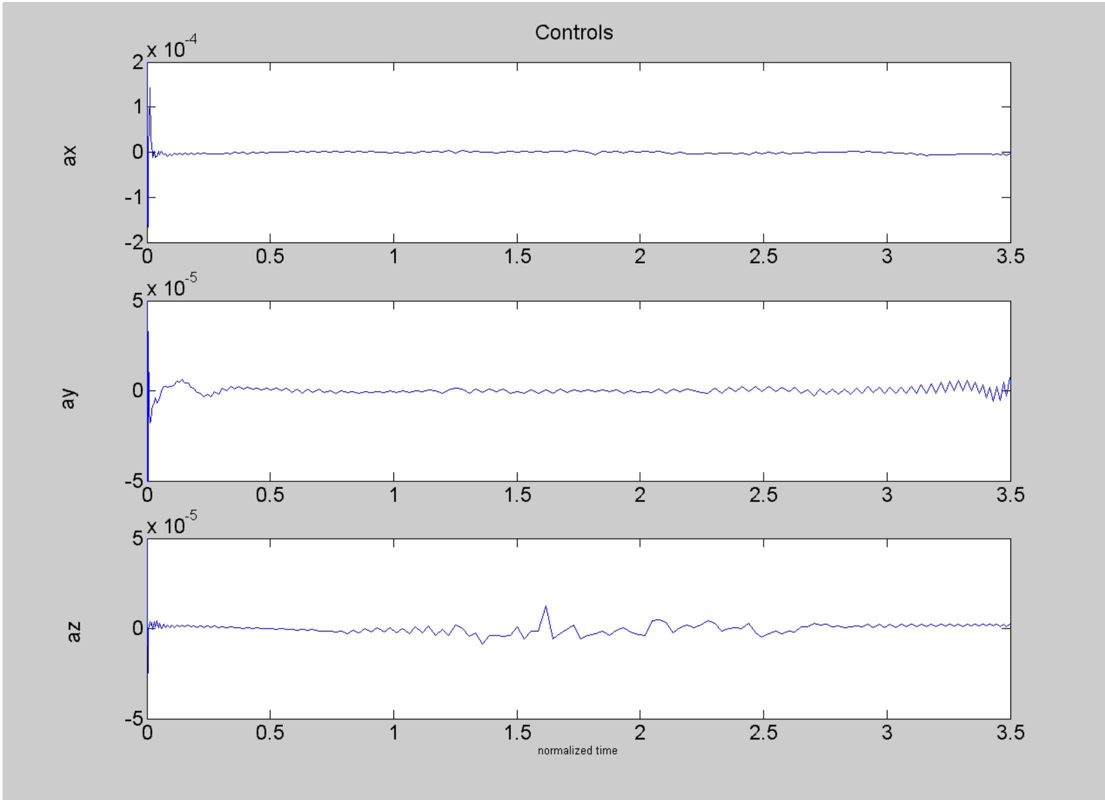

Figure 32. Controls for Unstable Orbit Solution about L2 Libration Point

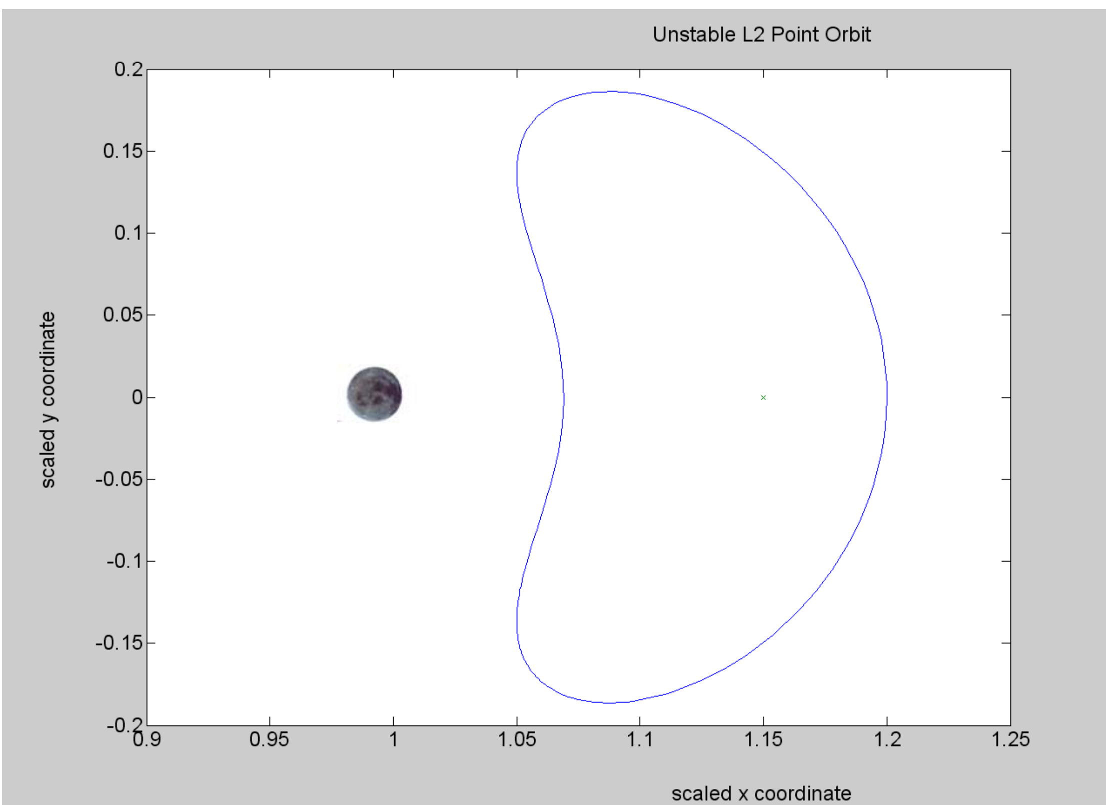

Figure 33. Unstable L2 Orbit with Respect to Moon

B. VALIDATION

The validity of the unstable point solution was conducted in the same manner as the stable solution. The control solution generated by the DIDO optimizer was propagated through the ODE 45 solver, with the linear interpolation of the controls was used in this case. Figure 34 shows the comparison between the propagator solution shown in red and the DIDO trajectories shown in blue. The error between the DIDO solution and the propagator was comparable to the stable solution error. The Hamiltonian is shown on the following page in Figure 35. Again, this solution was obtained by using an initial circle guess solution of 100 nodes, followed by a "bootstrapped" solution of 200 nodes.

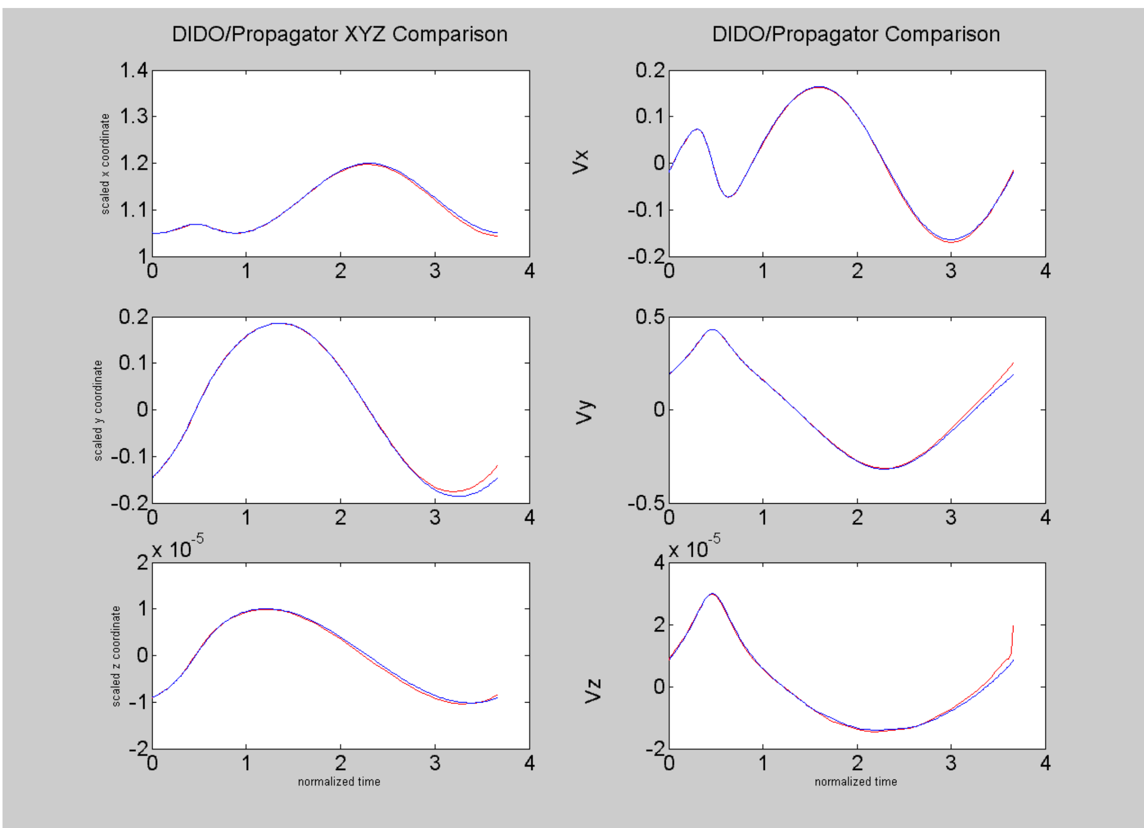

Figure 34. Unstable L2 Libration Point Propagator Comparison

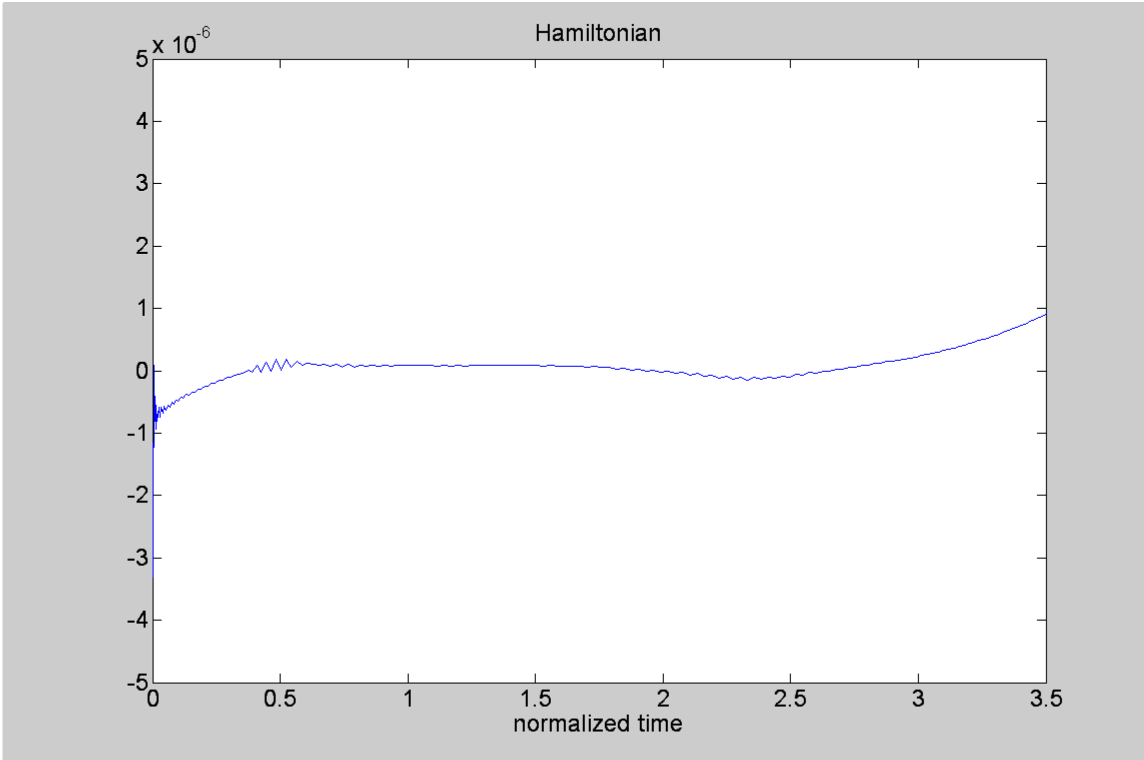

Figure 35. Hamiltonian for Unstable L2 Libration Point Solution

THIS PAGE INTENTIONALLY LEFT BLANK

VII. CONCLUSIONS AND FUTURE WORK

Libration points provide additional locations for spacecraft orbits with no obstructions or interruptions in coverage due to eclipse, which are observed in traditional orbits. The design of such orbits is particularly desirable for low thrust [Ref 21] vehicles since small thrust magnitudes on the order of 2 to 3 x 10^{-3} m/s^2 are required to maintain orbit. Unstable libration points demand more stringent control functions than the stable points, which are more sensitive to slight deviations and perturbations, would require accelerations on the order of 10^{-4} and 10^{-5} m/s^2.

Future work related to this thesis might include the incorporation and optimization of the departure trajectory from Earth orbit into a Halo orbit insertion, which would also be required to complete a mission to any libration point. Additionally, the design of a low thrust control system or model might be explored based on the requirements dictated by the controls of the DIDO optimization software for orbits about the libration points.

THIS PAGE INTENTIONALLY LEFT BLANK

LIST OF REFERENCES

1. M. Beckman, "Orbit Determination Issues for Libration Point Orbits," International Conference on Libration Point Orbits and Applications, Girona, Spain, 2002.

2. D. Dunham and R. Farquhar, "Libration Point Missions, 1978-2002," International Conference on Libration Point Orbits and Applications, Girona, Spain, 2002.

3. Website: http://stardust.jpl.nasa.gov/comets/ice.html "International Sun-Earth Explorer (ISEE-3)," November 2003.

4. Website: http://sohowww.nascom.nasa.gov/ "Solar Heliospheric Observatory (SOHO)," November 2003.

5. Website: http://lep694.gsfc.nasa.gov/waves/waves.html "WIND," December 2003.

6. Website: http://www.srl.caltech.edu/ACE/ "Advanced Composition Explorer (ACE)," November 2003.

7. Website: http://map.gsfc.nasa.gov/ "Microwave Anisotropy Probe (MAP)," November 2003.

8. Website: http://genesismission.jpl.nasa.gov/ "GENESIS," November 2003.

9. Website: http://sci.esa.int/science-e/www/area/index.cfm?fareaid=28 "DARWIN," November 2003.

10. O. Junge, J. Levenhagen, A. Seifreied, and M. Dellnitz, "Identification of Halo Orbits for Energy Efficient Formation Flying," Proceedings of the International Symposium Formation Flying, Toulouse, France, 2002.

11. T. Starchville and R. Melton, "Optimal Low-Thrust Trajectories to Earth-Moon L2 Halo Orbits (Circular Problem)," AAS 97-714, AIAA Astrodynamics Specialist Conference, Sun Valley, ID, 1997.

12. Emails between S. Infield (Stanford PhD candidate) and the author, November 2003.

13. W. Wiesel, *Spaceflight Dynamics*, McGraw-Hill, Inc., New York, New York, 1989.

14. D.A.Vallado, *Fundamentals of Astrodynamics and Applications*, Second Edition, El Segundo, CA, 2001.

15. R. Battin, *An Introduction to the Mathematics and Methods of Astrodynamics*, American Institute of Aeronautics and Astronautics, Inc., New York, New York, 1987.

16. J. J. Sellers, *Understanding Space*, McGraw-Hill, Inc., New York, New York, 1994.

17. S. Josselyn, "Optimization of Low Thrust Trajectories with Terminal Aerocapture," Engineer's Thesis, U. S. Naval Postgraduate School, Monterey, CA, June 2003.

18. I. M. Ross and F. Fahroo, "User's Manual for DIDO 2002: A MATLAB Application Package for Dynamic Optimization," *NPS Technical Report*, AA-02-002, Department of Aeronautics and Astronautics, Naval Postgraduate School, Monterey, CA June 2002.

19. S. Josselyn and I. M. Ross, "A Rapid Verification Method for the Trajectory Optimization of Reentry Vehicles," *Jounal of Guidance, Navigation and Control*, to appear.

20. I. M. Ross, *AA 3830 Class Notes*, Monterey, CA, Spring 2003.

21. G. Sutton and O. Biblarz, *Rocket Propulsion Elements*, John Wiley & Sons, New York, New York, 2001.

Various on-line resources for some figure art.

INITIAL DISTRIBUTION LIST

1. Defense Technical Information Center
   Ft. Belvoir, Virginia

2. Dudley Knox Library
   Naval Postgraduate School
   Monterey, California

3. Professor I. Michael Ross
   Naval Postgraduate School
   Monterey, California

4. Professor Don Danielson
   Naval Postgraduate School
   Monterey, California

5. Gina McCaine
   SWOSCOLCOM
   Newport, Rhode Island